PCR: Cx32-RT5, 5′-atgcacgtagcctcaccaacagcac-3′; Cx32-RT3, 5′-actcgtagccagcgagaaaagtcg-3′; murine β-actin-5′, 5′-gtaccacgggcattgtgatg-3′; and murine β-actin-3′, 5′-cgttctatcgtgtcgaagag-3′ (15).

Single-Dose Administration of MNU. Mice were randomly assigned to groups and individually housed. Immediately before use, MNU (Nakarai-Tesque Co. Ltd.) was dissolved in citrate buffer (0.01 *M* sodium citrate and 0.14 *M* NaCl, pH 5.5) and injected ip into the mice (25, 26).

Leukemogenicity Bioassay. Leukemogenicity was determined by a conventional whole-body bioassay and a transplantation bioassay (22). In the conventional whole-body assay, twelve 8-week-old Cx32-KO male mice ($Cx32^{-/Y}$) and ten wild-type littermates ($Cx32^{+/Y}$) were injected ip with MNU at 50 mg/kg body wt. In the transplantation bioassay, aliquots of single-cell suspension of the bone marrow (1×10^6 cells) from 8-week-old $Cx32^{-/Y}$ or $Cx32^{+/Y}$ male mice were injected into the tail vein of 8-week-old, 915-cGy–irradiated, wild-type female recipient mice. Only male mice were used as donors and only female mice were used as recipients to utilize the Y chromosome–specific sequence (a candidate testis-determining gene) for differentiating donor-derived neoplasms from recipient-derived neoplasms (27, 28). To study the effect of competitive repopulation on leukemogenicity, a group of mice was also injected with a mixture of cells, one half of which were Cx32-KO bone marrow cells and the other half wild-type bone marrow cells (mixture group). In this procedure, the numbers of CFU-S-9 transferred into each recipient mouse were 3.2 (wild type), 3.1 (mixture group), and 2.6 (Cx32-KO) $\times 10^2$. In this transplantation bioassay, bone marrow cells from Cx32-KO or wild-type mice were equally effective in protecting against the lethal dose of radiation, and bone marrow cellularity nearly reached that of the steady state after 4 weeks (data not shown). Four weeks after transplantation, 36 and 45 recipient mice were injected ip with MNU at 50 and 75 mg/kg body wt, respectively. The mice were supplied with water *ad libitum*. The mice in both the conventional leukemogenicity whole-body bioassay and in the transplantation bioassay were monitored throughout their lifetime at least twice daily. Those showing symptoms of advanced leukemia, such as anemia and palpable splenomegaly, were euthanized at the agonal period and then examined hematopathologically. Additionally, mice that died were subjected to gross and microscopic examinations (26).

Histopathological Examination. For the evaluation of hematopoietic malignancies caused by the injection of MNU in wild-type and Cx32-KO mice, mice from each group were sacrificed under ethyl ether anesthesia for necropsy. For the histopathological examination, all the visceral organs, including the thymus, spleen, sternum, and femoral bone marrow, were fixed in 4% neutral-buffered formalin for 24 hrs. The sternum and femoral bone marrow were decalcified in 7.5% formic acid for 72 hrs. After routine processing, paraffin-embedded sections were stained with hematoxylin and eosin and then examined histopathologically using a light microscope (22).

Immunohistochemical Staining. To confirm the cellular location of Cx32-positive progenitor cells, spleen colonies were examined by immunohistochemical staining with the anti-Cx32 antibody. Spleen sections containing colonies were fixed with 4% paraformaldehyde solution and embedded in paraffin for thin sectioning. The thin sections were then immunohistochemically stained with the anti-Cx32 antibody, a biotinylated secondary antibody, a horse anti-mouse IgG antibody, and streptavidin labeled with peroxidase to form the ABC complex with 3,3′-DAB.

Statistical Analyses. The data obtained were stored in a computer and processed for statistical analyses using the Kaplan-Meier method for survival curves and the log-rank test for their statistical significance. The Student *t*-test was used to evaluate the significance of differences in blood cell count, bone marrow cellularity, and the numbers of progenitor cells, CFU-GMs, CFU-S-9s, and CFU-S-13s between the wild-type group and the KO group. The incidence of hematopoietic neoplasms was evaluated by Fischer exact test. Differences with a P value <0.05 were considered significant.

Results

Expression of Cx32 in Hematopoietic Progenitor Cells and Its Function in Steady-State Hematopoiesis. *Expression of Cx32 in Hematopoietic Cells.* Figure 1A shows the expression of Cx32 in various lympho-hematopoietic tissues of wild-type mice. As previously reported (19), Cx32 was detected at the mRNA level only in the hepatic tissue by RT-PCR analysis, but was not detected in the spleen, bone marrow, and thymus.

Expression of Cx32 in Hematopoietic Spleen Colonies Developed from Progenitor Cells. We next studied Cx32 expression in colonies developed in the spleen of lethally irradiated wild-type recipient mice following injection of bone marrow cells from wild-type mice or Cx32-KO donor mice. Hematopoietic spleen colonies are rich in immature cells rather than in cells from peripheral blood or unfractionated bone marrow (24). As shown in Figure 1B, the expression of Cx32 detected by RT-PCR analysis was observed only in the hematopoietic spleen colonies but derived from wild-type bone marrow cells (a1 through a3), not in the colonies derived from Cx32-KO bone marrow cells (c1 and c2). Cx32 expression also was detected in the spleen colonies in Cx32-KO recipient mice repopulated with wild-type bone marrow cells (b1 and b2).

Immunohistochemical staining with the anti-Cx32 antibody was carried out to examine the hematopoietic spleen colonies originating from bone marrow cells from wild-type mice and Cx32-KO mice (Fig. 2). A colony originating from a wild-type bone marrow cell (Fig. 2Aa) shows mild and mottled staining in beige, whereas a colony originating from Cx32-KO bone marrow cells are negative

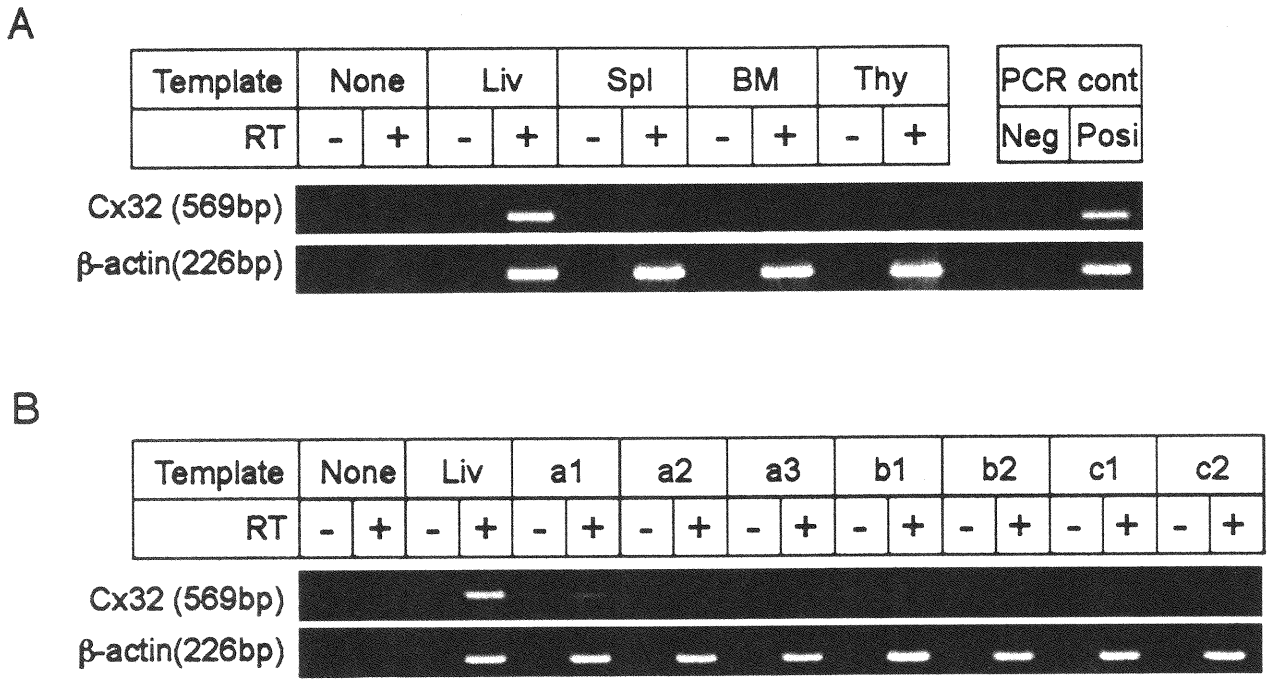

Figure 1. Expression of Cx32 in the lympho-hematopoietic tissues and hematopoietic spleen colonies. (A) Expression of Cx32 in lympho-hematopoietic tissues. Total RNAs were extracted for RT-PCR from the liver (Liv), spleen (Spl), bone marrow (BM), and thymus (Thy) of wild-type mice. Note that Cx32 expression was not detected in the spleen, bone marrow, or thymus, but was detected in the liver, a positive control (see *Materials and Methods*). PCR: for "Neg" lane and "Posi" lane, no template and whole genome extracted from the tail were loaded, respectively. RT(+) and RT(–): With or without Avian reverse transcriptase, 2.5 U/20 μl, respectively (see *Materials and Methods*). (B) Expression of Cx32 in hematopoietic spleen colonies (see *Materials and Methods*). Lethally irradiated wild-type mice were injected with bone marrow cells from wild-type or Cx32-KO donor mice. After 9 days, total RNAs extracted from individual hematopoietic spleen colonies derived from wild-type bone marrow cells or those from Cx32-KO bone marrow cells were reverse transcribed followed by PCR and then loaded (a1–a3, c1 and c2). Total RNAs extracted from colonies derived from wild-type bone marrow cells removed from the lethally irradiated Cx32-KO recipient mice followed by repopulation with wild-type bone marrow cells were similarly loaded (b1 and b2).

in staining (Fig. 2Ba and b). Interestingly, in a colony observed at a higher magnification (Fig. 2Ab), cells from wild-type mice positively stained by the anti-Cx32 antibody were only scattered in the outer boundary of spleen colonies (circled by dotted line in Fig. 2Aa and arrows in Fig. 2Ab), indicating that the incidence of primitive progenitor cells was still low in the spleen colonies.

Expression of Cx32 in Hematopoietic Stem Cell Compartment. We then next determined whether Cx32-positive cells are consistently found in the HSC compartment. First, the $lin^-c\text{-}kit^+$ HSC-enriched fraction was obtained by the combination of immunobead-density gradient separation for depleting lineage-positive cells and immunomagnetic bead separation for selecting $c\text{-}kit^+$ cells, followed by flow cytometric analysis using the anti-Cx32 antibody. As a result, the separated $lin^-c\text{-}kit^+$ HSC fraction was 0.25% with respect to the original unfractionated wild-type bone marrow cells. Figure 3 shows the flow cytometric distribution of the $lin^-c\text{-}kit^+$ HSC-enriched fraction (Fig. 3B) compared with original unfractionated cells (Fig. 3A) from both wild-type bone marrow cells (the horizontal axis for lineage markers and the vertical axis for c-kit). In Figure 3B, the percentage of $lin^-c\text{-}kit^+$ compartment (HSC compartment) indicated by an asterisk is 90.2% of the $lin^-c\text{-}kit^+$ HSC-enriched preseparated fraction. Furthermore, the number for $lin^-c\text{-}kit^+$ compartment (asterisk in Fig. 3B) is 106.9 times enriched compared to the fraction of the original unfractionated bone marrow cells, as shown in the enclosed corresponding square (Fig. 3A). To determine which fraction Cx32-positive cells belong to, bone marrow cells from wild-type mice and Cx32-KO mice were stained with lineage-PerCP, c-kit–PE, and Cx32-FITC with or without the $lin^-c\text{-}kit^+$ HSC enrichment. In Figure 3C, 28.8% of the $lin^-c\text{-}kit^+$ fraction of wild-type bone marrow cells was found to be Cx32 positive (unshaded profile) compared with the same fraction of bone marrow cells obtained from Cx32-KO mice (shaded profile), which was used as the negative control. Together with frequency data of the $lin^-c\text{-}kit^+$ HSC-enriched fraction, Cx32-positive cells are calculated nearly 0.27% with respect to the original unfractionated whole bone marrow cells.

Whether the mature cell fraction, a $lin^+c\text{-}kit^-$ fraction, contains Cx32-positive cells, the fraction of wild-type bone marrow cells (unshaded profile) is compared to that of the control profile from Cx32-KO mice (shaded profile), as shown in Figure 3D. Since both fractions are nearly identical, few cells may be positive for Cx32 in the $lin^+c\text{-}kit^-$ fraction (0.27% of the $lin^+c\text{-}kit^-$ fraction; Fig. 3D).

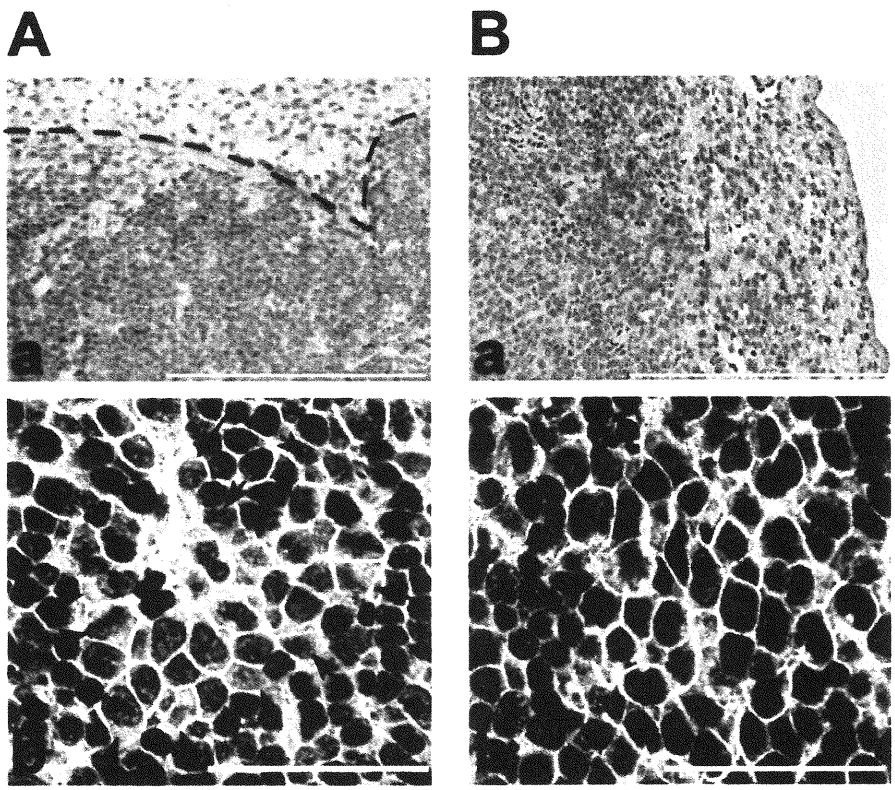

Figure 2. Cells in spleen colonies immunohistochemically stained with anti-Cx32 antibody. (A) Spleen colonies derived from wild-type bone marrow cells (a and b). (B) Cx32-KO bone marrow cells (i.e., control for negative staining; subpanels a and b). As shown in Aa and Ba, cells from spleen colonies were found positively stained with a mottled pattern in the former figure and negatively stained in the latter figure. The positively stained cells are located only in the outer boundary of the colony. Dotted line in Aa indicates border of the colony. Ab and Bb show a higher magnification of spleen colonies derived from wild-type mice and Cx32-KO mice, respectively. As shown in Ab, a colony was a mottled pattern with positively stained cells (arrows) in beige. Bb shows the negative control. Spleens were stained with the anti-Cx32 antibody and with the biotinylated secondary antibody, horse anti-mouse IgG antibody, and streptavidin labeled with peroxidase. Bars indicate 200 μm in Aa and Ba, and 25 μm in Ab and Bb.

Cx32-positive cells are 0.0093% with respect to the original unfractionated whole–bone marrow cells (data not shown).

Function of Cx32 in the Steady-State Hematopoiesis. The steady-state hematopoiesis of wild-type mice was compared to that of Cx32-KO mice. Figure 4A shows the comparison of the absolute body weight, splenic weight, and cellularity of the bone marrow. There were essentially no differences in any of these parameters between wild-type mice and Cx32-KO mice. However, the number of white blood cells and that of platelets were significantly different between wild-type mice and Cx32-KO mice, as shown in Figure 4B. Regarding the decrease in the number of white blood cells, there was no trend toward decrease between numbers of lymphocytes and neutrophils. Moreover, there was no difference in the number of red blood cells. Regarding the number of CFU-GMs, there was a significantly lower number of progenitor cells per unit number of bone marrow cells in Cx32-KO mice than in wild-type mice. Hematopoietic progenitor cells that form CFU-S-9s are considered to be more mature than those that form CFU-S-13s (29, 30). As shown in Figure 4C, in terms of the maturation stages from CFU-S-13 and CFU-S-9 to CFU-GM, the number of all of the hematopoietic progenitor cell compartments of Cx32-KO mice was lower than that of the wild-type mice. Therefore, the present study clearly showed that Cx32 deficiency induced an impaired hematopoiesis specifically in the immature progenitor cell fraction, and changes in differentiated cells may be a reflection of those in immature cells. Thus, Cx32 is assumed to be required for the maintenance of immature hematopoietic progenitor cells.

Function of Cx32 During Growth of Hematopoietic Progenitor Cells. Although the stromal cell–dependent connexin Cx43 is known to function in cultured stromal cells (12, 13), few cells were positive in anti-Cx32 antibody in the bone marrow. Thus, one question is to answer is whether the hematopoietic defect observed in Cx32-KO mice exists solely in hematopoietic progenitor cells, or also in stromal cells. Accordingly, to examine whether Cx32 deficiency has a negative effect on hematopoiesis in stromal cells of Cx32-KO mice, lethally irradiated wild-type mice and Cx32-KO mice were repopulated with bone marrow cells from wild-type mice or Cx32-KO mice. Results from four different combinations are shown in Figure 5.

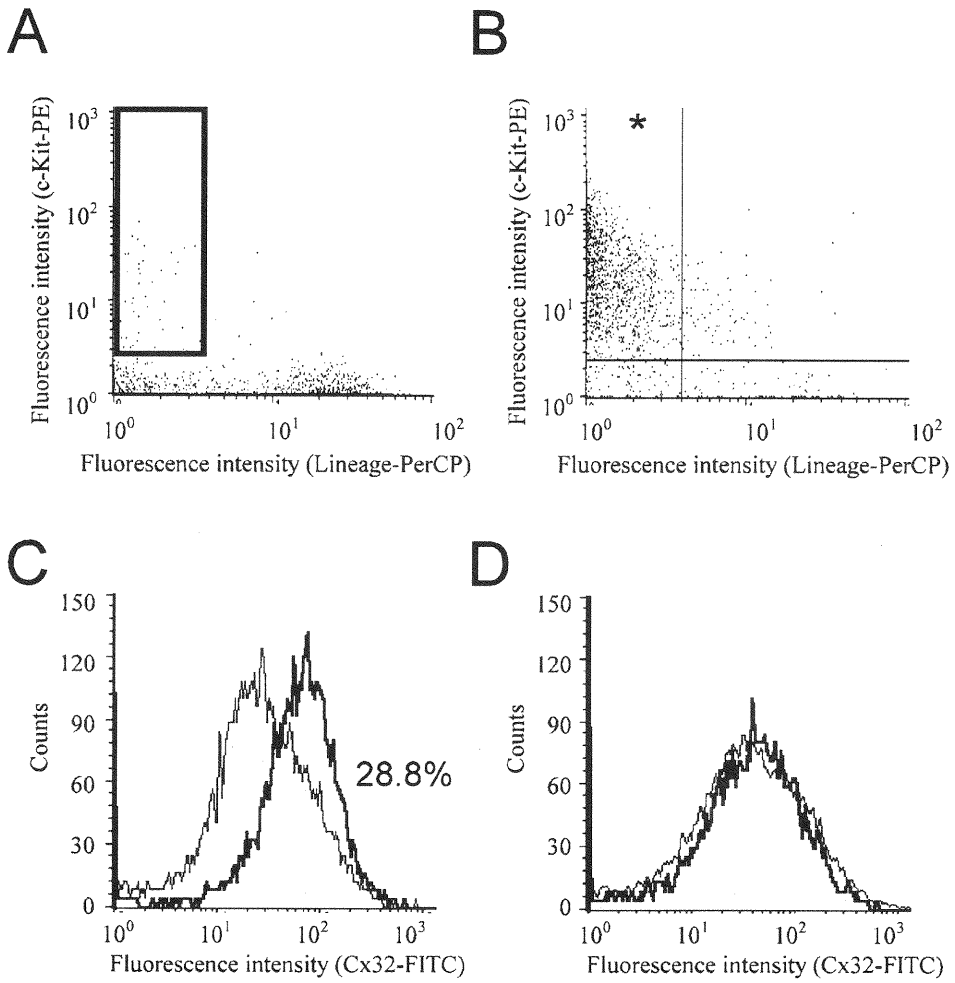

Figure 3. Flow cytometric analyses for lin$^-$c-kit$^+$ HSC-enriched fraction and lin$^-$c-kit$^+$ Cx32-positive cells from wild-type mice. Flow cytometry after bone marrow cell separation carried out by a combination of the immunobead-density gradient separation and the immunomagnetic bead separation. (A) Unseparated bone marrow cells. (B) Bone marrow cells fractionated by combination of the immunobead-density gradient separation for eliminating lineage marker positive cells and the immunomagnetic bead separation for c-kit$^+$ cells. The vertical axis in both figures indicates fluorescence intensity for the PE-labeled anti–c-kit antibody, and the horizontal axis indicates fluorescence intensity for Per-CP–labeled streptavidin for biotinylated lineage antibodies. The vertical and horizontal lines in panel B indicate the negative and positive borders of fluorescence intensity. The asterisk in panel B indicates the targeted lin$^-$c-kit$^+$ compartment and HSC compartment. Note that the corresponding area of the asterisk in panel B is indicated by the square box in panel A. (C and D) Histogram of the FITC-labeled anti-Cx32 antibody. The lin$^-$c-kit$^+$ fraction (C) and the lin$^+$c-kit$^-$ fraction (D) for wild-type bone marrow cells (open profile with bold line) and the same fraction for Cx32-KO bone marrow cells (shaded profile), a negative control. Cx32-positive fraction in panel C calculated for the lin$^-$c-kit$^+$ fraction in wild-type bone marrow cells is 28.8%.

Regardless of the expression of Cx32 in stromal cells in either Cx32-KO recipient mice or wild-type recipient mice, there were no statistically significant differences in the number of spleen colonies (CFU-S-9s) between the pair of groups that received either wild-type bone marrow cells (Fig. 5A, two left columns) or Cx32-KO bone marrow cells (Fig. 5A, two right columns). Thus, Cx32 deficiency in progenitor cells is concluded as a major factor that is responsible for the production of a significantly small number of colonies. As observed in Figure 4C, it is confirmed that the number of colonies is larger when donor bone marrow cells are from wild-type mice than when they are from Cx32-KO mice.

In Figure 5B, the size of spleen colonies in each group is shown. Significantly smaller colonies were observed in the three groups in which recipient mice, donor bone marrow cells, or both were from Cx32-KO mice rather than in the group in which both recipient mice and donor bone marrow cells were from wild-type mice (Fig. 5B, open column). Because there was no significant difference in size between groups repopulated with Cx32-KO bone marrow cells, the major factor for producing small colonies (Fig. 5B, two right columns) also is assumed to be responsible for Cx32 deficiency in donor progenitor cells, rather than any factor from stromal cells. Concerning the group that received wild-type bone marrow cells (Fig. 5B, the second

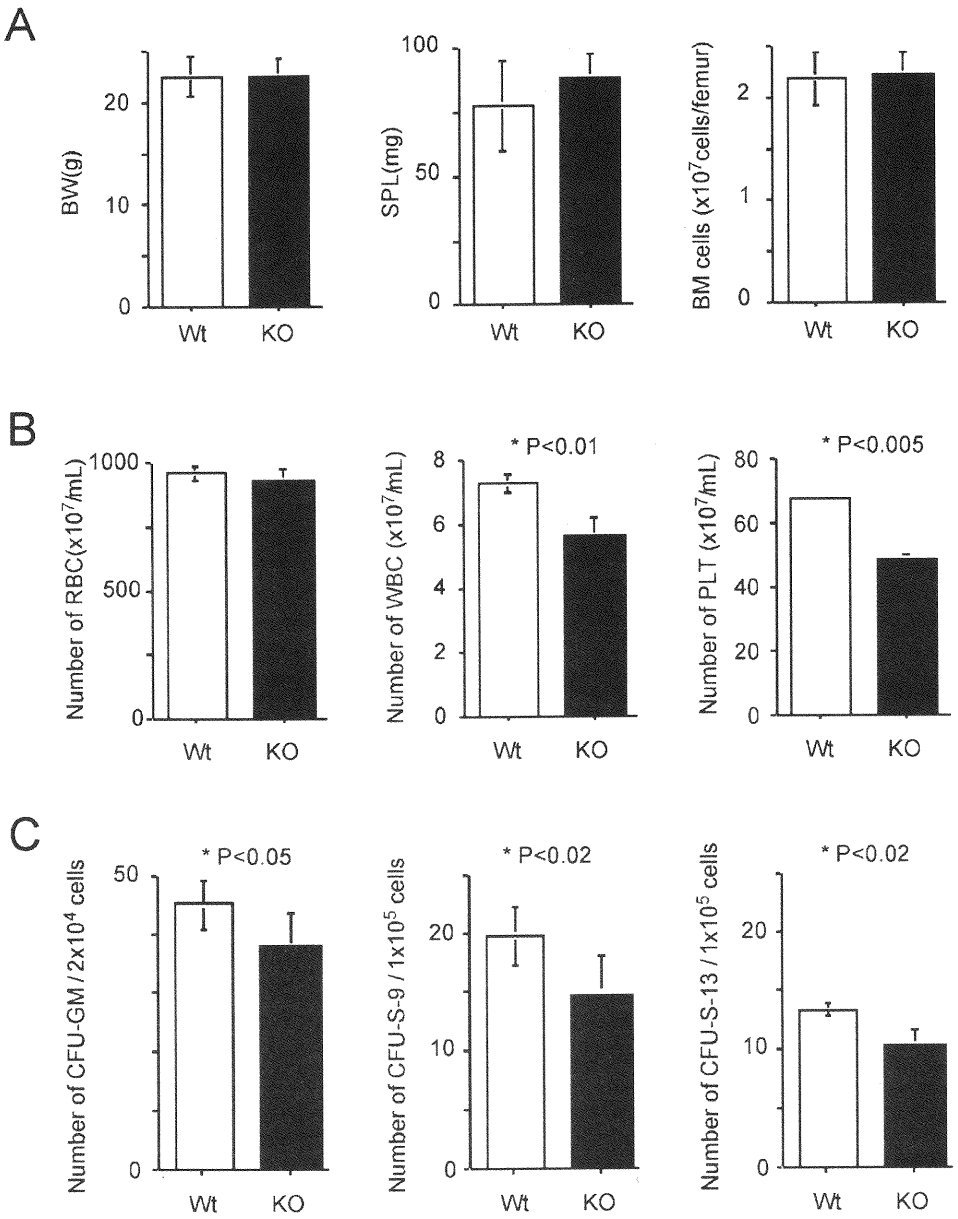

Figure 4. Parameters associated with steady-state hematopoiesis. Row A: from left, body weight (BW), splenic weight (SPL), and bone marrow cellularity (BM cells; $n = 6$ in each genotype). Row B: from left, numbers of peripheral blood cells—red blood cells (RBCs), white blood cells (WBCs), and platelets (PLTs; $n = 6$ for each genotype). Row C: from left; numbers of hematopoietic progenitor cells in steady-state CFU-GMs, hematopoietic progenitor cells for CFU-S-9s, and those for CFU-S-13s. Three donor mice were used for each genotype, and six mice were used for each recipient group. Open box, wild type; solid box, Cx32-KO; vertical bar, standard deviation of the mean. *Difference between wild-type and Cx32-KO mice is significant (*P* values are indicated in each figure).

shaded column from the left), Cx32-KO mice produced significantly smaller colonies due to as yet undetermined reasons.

Regeneration Potency of Bone Marrow Cells from Cx32-KO Mice and Wild-Type Mice. Treatment with 5-fluorouracil (5-FU) induces a temporary arrest of hematopoietic progenitor cell proliferation, except in the very immature hematopoietic progenitor cell compartment (30–32), in which mature hematopoietic progenitor cells are killed, whereas immature dormant HSCs selectively survive. The number of CFU-GMs per unit number of bone marrow cells was counted for 2 weeks after the 5-FU treatment. As shown in Figure 6, the number of CFU-GMs in both wild-type mice and Cx32-KO mice increased rapidly after 5-FU treatment; however, the increase in the number of CFU-GMs seemed to be delayed in Cx32-KO mice compared with that of wild-type mice.

Experimental Leukemogenesis: Whole-Body

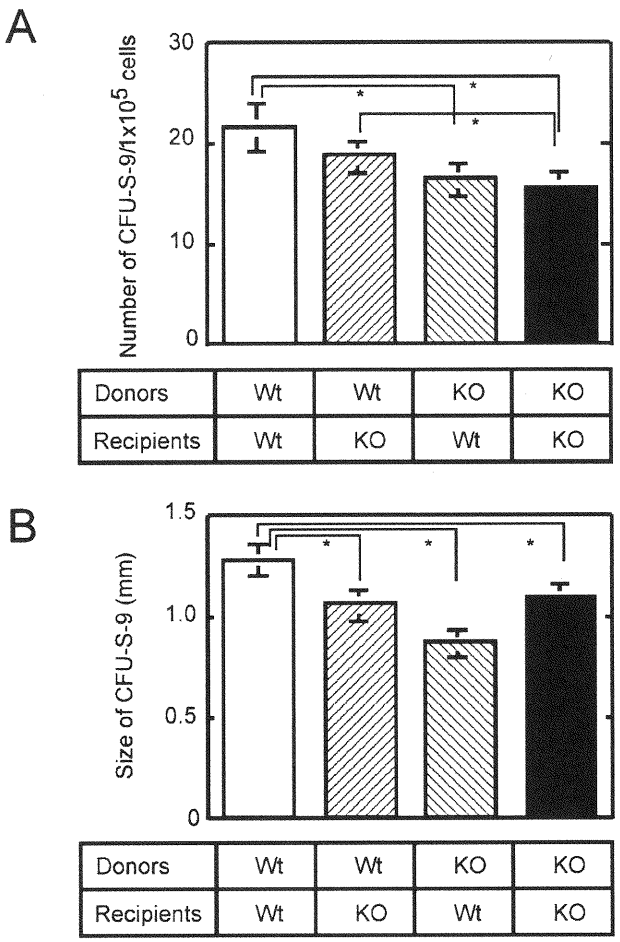

Figure 5. Number and size of CFU-Ss assayed in four different combinations between donors, either wild-type or Cx32-KO bone marrow cells, and lethally irradiated recipients, either wild-type or Cx32-KO mice. (A) Number of CFU-S-9s. (B) Size of CFU-S-9s. *Differences between each bar connected with a line are significant ($P < 0.05$); three donor mice were used for each genotype, and six mice were used for each recipient group.

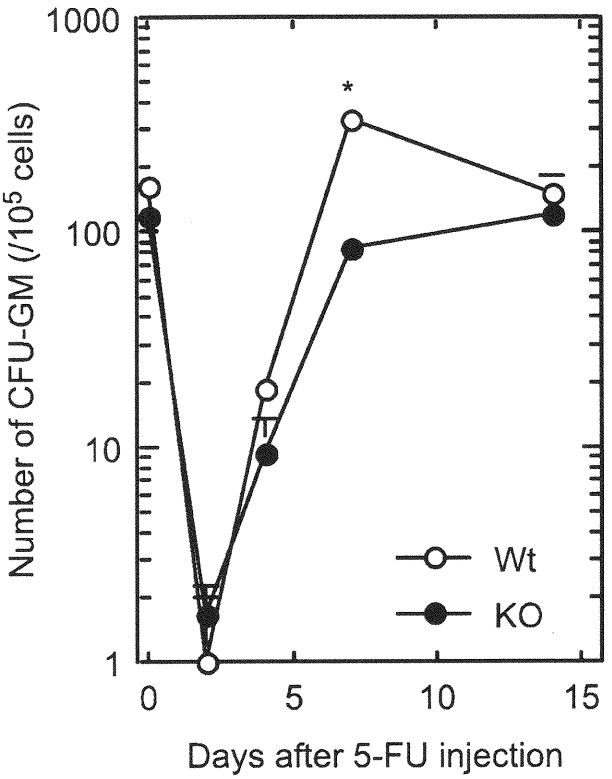

Figure 6. Changes in number of CFU-GMs in femoral bone marrow cells in wild-type or Cx32-KO mice (days after a single dose of 5-FU, iv, 150 mg/kg body wt). Open circle, wild type; closed circle, Cx32-KO. *Seven days after 5-FU injection, at which time the difference between the wild-type and Cx32-KO mice was significant ($P < 0.05$); three mice each were used for each data point).

Bioassay and the Transplantation Bioassay With or Without Cx32. *Cx32-KO Hematopoietic Progenitor Cells and Leukemogenesis.* A high incidence of hematopoietic neoplasms was observed during the MNU-induced leukemogenesis in Cx32-KO mice. The survival curves of the mice of each group showed that the MNU-treated mice, regardless of genotype, died much earlier because of MNU-induced hematopoietic malignancies and other diseases (Fig. 7A). Untreated control mice, regardless of genotype, gradually started to die 400 days after the treated groups received an MNU.

The percentage of incidences of hematopoietic malignancies in mice treated with MNU, both wild-type and Cx32-KO, and mice in both nontreated control groups are shown in Figure 7B. When Cx32 was knocked out, the incidence of hematopoietic malignancies started to increase rapidly 100 days after MNU treatment (closed squares), which exceeded the incidence of hematopoietic malignancies in wild-type mice (50.0%), and reached 91.7% ($P < 0.05$ by Fischer exact test). The incidence of hematopoietic neoplasms in nontreated groups of both wild-type and Cx32-KO mice as reference groups increased gradually, reaching 40.0% for the wild-type mice and 33.3% for Cx32-KO mice. Concomitantly, hepatomas developed in both groups of mice after 664 days of age, and the incidence in Cx32-KO mice was higher than that in wild-type mice, although it was statistically less significant (33.3% and 10.0%, respectively; data not shown).

Assay of Leukemogenicity: The Transplantation Assay in Cx32-KO Bone Marrow Cells and Wild-Type Bone Marrow Cells. Because the incidence of hematopoietic malignancies was significantly high in Cx32-KO mice (Fig. 7B), but the development of hematopoietic malignancies was interfered with by malignancies from other tissues and organs due to competitive risk of the tumorigenicity (data not shown and Ref. 22), lethally irradiated same wild-type mice were repopulated with either bone marrow cells from wild-type mice or Cx32-KO mice, and the development of hematopoietic neoplasms after a single dose of MNU was observed under the same recipient

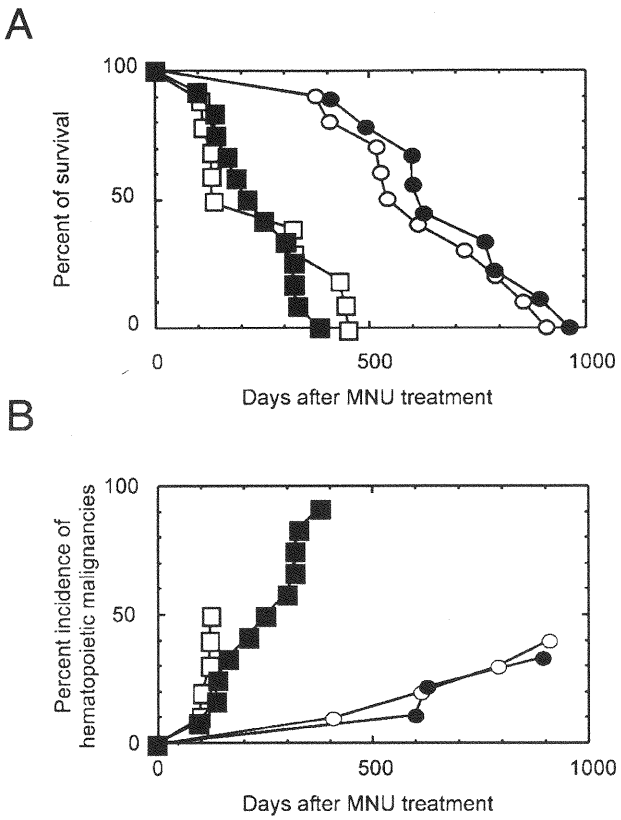

Figure 7. Whole-body assay of hematopoietic malignancies by a single dose of MNU at 50 mg/kg body wt. (A) Survival fraction. (B) Cumulative incidences of hematopoietic malignancies in Cx32-KO mice or wild-type mice with or without a single ip injection of MNU. Open circle, wild type without MNU injection, 10 mice; open square, wild type with MNU injection, 10 mice; closed circle, Cx32-KO without MNU injection, 9 mice; closed square, Cx32-KO with MNU injection, 12 mice.

conditions (the transplantation assay). However, few differences in survival time and incidence of neoplasms were observed between mice repopulated with wild-type bone marrow cells and those repopulated with Cx32-KO bone marrow cells (data not shown).

Competitive Assay of Leukemogenicity Between Cx32-KO Bone Marrow Cells and Wild-Type Bone Marrow Cells. A mixed population of bone marrow cells from Cx32-KO and wild-type mice was injected into lethally irradiated wild-type mice, and the incidence of hematopoietic malignancies competitively caused by bone marrow cells from Cx32-KO mice and those from wild-type mice was determined under the same *in vivo* conditions of the recipient (the competitive assay). Figure 8 shows the incidences of hematopoietic malignancies in mice that received a single dose of MNU at either 75 mg/kg body wt (dark squares) or 50 mg/kg body wt (medium squares), compared with the nontreated control (light squares), which are plotted against the days after MNU treatment. The incidence of hematopoietic malignancies of the 75 mg/kg body wt MNU-treated group reached 88.9%, whereas that of

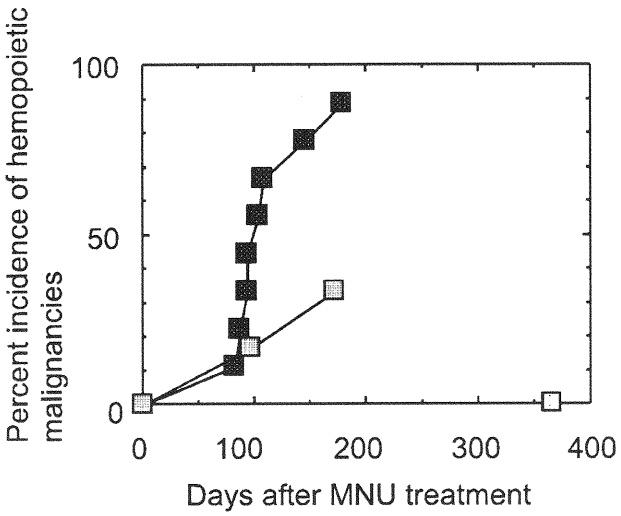

Figure 8. Competitive bone marrow transplantation bioassays repopulated with mixture of bone marrow cells from wild-type and Cx32-KO mice, followed by a single dose of MNU. Cumulative incidences of hematopoietic malignancies in the group repopulated with the mixture cells followed by a single ip injection of MNU at 50 or 75 mg/kg body wt. Light square, vehicle treatment; medium squares, 50 mg treatment; dark squares, 75 mg treatment.

the 50 mg/kg body wt MNU-treated group reached 33.3%. The incidences of hematopoietic neoplasms that were observed in the competitive assays are shown in Table 1. In the mice treated with MNU at 50 mg/kg body wt and in those treated with 75 mg/kg body wt, two and eight hematopoietic neoplasms developed, respectively.

Samples from these neoplasms were analyzed for their genotype to determine whether the neoplasms originated from bone marrow cells of wild-type mice or Cx32-KO mice (Fig. 9). In Figure 9, lanes 1, 2, 4, 5, 6, 8, and 9 show the presence of the gene inserted for the knockout strategy; thus, the neoplastic samples in these lanes were identified as having originated from bone marrow cells of Cx32-KO mice. The origins of the hematopoietic neoplasms are shown in Table 1. The results show that the malignancies originated from the bone marrow cells of Cx32-KO mice in two of two leukemias in the 50 mg/kg body wt MNU-treated group, and in seven of eight leukemias in the 75 mg/kg body wt MNU-treated group.

Discussion

The role of Cx32 in steady-state hematopoiesis and its potential protective role of prevention during leukemogenesis were analyzed in this study. In this study we demonstrated for the first time that a Cx gene, namely, the Cx32 gene, is expressed in hematopoietic stem/progenitor cells, and in the case of Cx32-KO mice, the regeneration of bone marrow after chemical abrasion was clearly delayed, which suggests a beneficial role of Cx32 in the regeneration. Furthermore, the incidence of MNU-induced leukemia was

Table 1. Transplantation Bioassays for Repopulation with Mixture of Bone Marrow Cells Followed by Induction of Tumor by MNU, and Genotyping of Tumor Origin

		Tumor origin, no. (%)	
Dose of MNU	No. of tumors	Wild type	KO
50 mg/kg body wt	2	0 (0)	2 (100)
75 mg/kg body wt	8	1 (12.5)	7 (87.5)

clearly high in Cx32-KO mice after a single administration of MNU, as shown not only in the whole-body assay (Fig. 7) but also in the competitive repopulation assay using bone marrow cells from Cx32-KO and wild-type mice (Figs. 8 and 9). These results are compatible with the observation of epithelial tumorigenesis in the liver and lungs observed in the same Cx32-KO strain (9), and this is the first observation in leukemogenesis.

Various Cxs are expressed in stromal cells of the fetal liver (Cxs 43, 45, 30.3, 31, and 31.1) and bone marrow (Cxs 43, 45, and 31; Ref. 13). However, the contribution of Cxs to hematopoiesis was found only on the basis of the effect of Cxs *via* stromal cell dependence; consequently, no Cxs were previously found in hematopoietic stem cells and/or progenitor cells (16). For us this is interesting, because hematopoietic progenitor cells possess morphologic evidence as well as functional evidence for cellular communication with each other (33, 34). Interestingly, in our recent study, Cx32-KO mice exposed to benzene showed a hematopoietic impairment; however, the site of this impairment was not identified in either hematopoietic progenitor or stromal cells (15).

Thus, we first determined whether hematopoietic progenitor cells express Cx32 molecules; however, as reported elsewhere, Cx32 is not detected in the bone marrow (Fig. 1A and Refs. 15 and 19). Interestingly, hematopoietic spleen colonies derived from hematopoietic progenitor cells were found to express Cx32 (Fig. 1B). This observation was further supported by the immunohistochemical reaction of cells in the colonies to the anti-Cx32 antibody, in which Cx32-positive cells were only scattered along the border of each colony (Figs. 2Aa and b). Furthermore, flow cytometry using the anti-Cx32 antibody after performance of the combination of immunobead-density gradient separation and the immunomagnetic bead separation showed that the Cx32-positive fraction was found to belong to the HSC compartment and was calculated as only 0.27% with respect to the unseparated bone marrow cells (Fig. 3). These findings may be in good agreement with a previous report of the absence of Cx32 expression in the bone marrow tissue (13). A hematopoietic disadvantage in progenitor cells associated with Cx32 deficiency was further evident, because all progenitor cells from the bone marrow of Cx32-KO mice showed a ~20% decrease in numbers of CFU-S-13s, CFU-S-9s, and CFU-GMs. Thus, it can be concluded that Cx32 is required for maintaining normal hematopoiesis, specifically during the maturation of hematopoietic stem cells to the progenitor cells.

However, whether Cx32 also is functional in differentiated mature blood cells is questionable, despite the observation that the numbers of white blood cells and platelets were significantly lower in the peripheral blood of the Cx32-KO mice than in the wild-type mice (Fig. 4B). It is of interest to calculate a probability of Cx32-positive cells based on this ratio of those Cx32-positive bone marrow cells out of the $lin^{+}c\text{-}kit^{-}$ fraction; that is, only 0.0093% with respect to that of unfractionated original bone marrow cells (data not shown). Because our repeated analyses failed to detect Cx32 expression in mature blood cells, the decreased numbers of white blood cells and platelets in the Cx32-KO mice are regarded as a reflection of the shortage of immature progenitor cell compartments due to the lack of Cx32 at the level of stem cells and progenitor cells.

The bone marrow transplantation in different combinations of the donor and recipient, which was repopulated with bone marrow cells from either wild-type mice or Cx32-KO mice, showed a small number of spleen colonies in the groups repopulated with Cx32-KO bone marrow cells. Interestingly, as shown in Figure 5B, colonies derived from the same Cx32-KO bone marrow cells showed significantly smaller colonies regardless of the genotype of recipients—that is, wild-type or Cx32-KO mice—presumably owing to

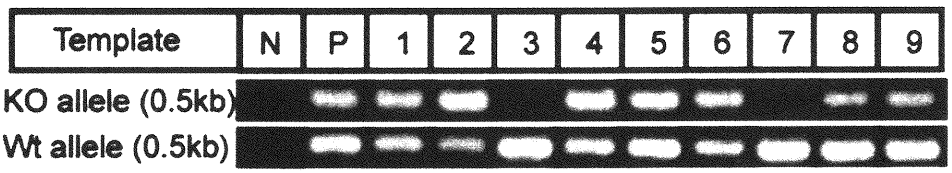

Figure 9. Genotyping of hematopoietic neoplasms whose origin was identified by genomic PCR. N, negative control for PCR without DNA; P, positive control for PCR using genomic DNA from the $Cx32^{-/-}$ hepatic tissue. Lanes 1–9, DNA extracted from hematopoietic neoplasms that developed during assay of bone marrow transplantation. Lane 3, control neoplasm that developed in mouse repopulated with wild-type bone marrow cells. Lane 4, control neoplasm that developed in mouse repopulated with Cx32-KO bone marrow cells. Lanes 1, 2, and 5–9, neoplasms that developed in mice repopulated with a mixture of bone marrow cells from wild-type and Cx32-KO mice. Note that lane 7 has a faint band for the KO allele, which shows an additional simultaneous expression band from the repopulated normal hematopoietic cells. For lanes 1, 2, 5, 6, 8, and 9, the tumors arising from Cx32-KO bone marrow cells show double bands, namely a Wt allele and another allele for KO strategy. Intensities of these bands are identical compared with that of lane 4.

the lack of Cx32 expression in the hematopoietic progenitor cells (shaded column second from the right vs. closed column far right). The reason why a small size of colonies observed in the Cx32-KO recipient mice received wild-type bone marrow cells cannot be answered in the present study. It is possible that Cx32 deficiency in combination with a lethal dose of whole-body irradiation for the bone marrow transplantation induces an unknown synergistic damage. Our previous observation that Cx32-KO mice treated repeatedly with a dose of benzene by inhalation showed a severe chemical-induced persistent pulmonary injury (15) may be relevant to the present observation. Stem cell regeneration after chemical abrasion with 5-FU was delayed in Cx32-KO mice (Fig. 6), which indicates that early recovery of mice also requires the growth of hematopoietic progenitor cells expressing Cx32. This is compatible with the observation of transgenic mice expressing a dominant-negative mutant of Cx32, which showed a notably delayed recovery after partial hepatectomy (5).

The role of Cx32 is associated with the prevention of carcinogenicity, as an initiation of leukemogenicity was preferentially induced in Cx32-KO mice by a single dose of MNU; thus, Cxs likely have a protective function against leukemogenicity, specifically for the initiation of the carcinogenic process. Phenotypically, the results are compatible with the observation that spontaneous hepatic tumors and diethyl-nitrosamine–induced hepatic tumors tended to develop in Cx32-KO mice compared with wild-type mice (9). Furthermore, radiation-induced hepatocarcinogenesis and diethyl-nitrosamine–induced pulmonary tumorigenesis showed a high frequency of tumorigenesis in Cx32-KO mice (35, 36), which also is compatible with the results of the present study.

Why does the lack of Cxs result in more frequent carcinogenesis? Why was the incidence of leukemogenesis higher in Cx32-KO mice (Fig. 7B, closed squares)? Furthermore, why did leukemogenicity in the wild-type mice appear earlier than that in Cx32-KO mice, although the total incidence remains lower by about 50% (Fig. 7B, open squares) than in the Cx32-KO mice (Fig. 7B, open squares vs. closed squares, respectively). The present study implies that Cx32-KO mice showed a high frequency of leukemogenesis due in part, to a possible suppression of apoptosis of hematopoietic progenitor cells after exposure to chemical carcinogens, and thereby the initiation of leukemogenicity was induced frequently in Cx32-KO mice. Cx32 is, therefore, surmised to protect hematopoietic progenitor cells from leukemogenic triggers in the wild-type mice.

The present competitive assay clearly showed that Cx32-KO bone marrow cells have a higher risk of becoming leukemogenic. The above-mentioned findings in this study imply that Cxs play an essential role in tumor suppression, although a temporary disconnection of Cxs induced by so-called carcinogenic promoter chemicals might induce an independent growth of possible neoplastic candidates, which may, however, eventually undergo apoptosis or be enclosed by cells with recovered Cx function.

Lastly, our results indicate that the risk of developing leukemia in patients with X chromosome–linked Cx32 deficiency, called Charcot-Marie-Tooth syndrome, might not be incidental.

This study is dedicated to the late Dr. Eugene P. Cronkite for his fifth-year memorial. We thank Dr. Y. Kawasaki, Dr. K. Sai, Ms. E. Tachihara, Ms. N. Moriyama, Ms. Y. Shinzawa, Ms. Y. Usami, Mr. K. Terasaka, and Mr. Morita for excellent technical assistance, and Ms. N. Kikuchi, Ms. M. Yoshizawa, and Ms. M. Hojo for secretarial assistance.

1. Loewenstein WR. Junctional intercellular communication and the control of growth. Biochim Biophys Acta 560:1–65, 1979.
2. Wilson MR, Close TW, Trosko JE. Cell population dynamics (apoptosis, mitosis, and cell-cell communication) during disruption of homeostasis. Exp Cell Res 254:257–268, 2000.
3. Bruzzone R, White TW, Paul DL. Connections with connexins: the molecular basis of direct intercellular signaling. Eur J Biochem 238:1–27, 1996.
4. Trosko JE, Chang CC, Madhukar BV. Modulation of intercellular communication during radiation and chemical carcinogenesis. Radiat Res 123:241–251, 1990.
5. Dagli ML, Yamasaki H, Krutovskikh V, Omori Y. Delayed liver regeneration and increased susceptibility to chemical hepatocarcinogenesis in transgenic mice expressing a dominant-negative mutant of connexin32 only in the liver. Carcinogenesis 25:483–492, 2004.
6. Mesnil M. Connexins and cancer. Biol Cell 94:493–500, 2002.
7. King TJ, Gurley KE, Prunty J, Shin JL, Kemp CJ, Lampe PD. Deficiency in the gap junction protein connexin32 alters p27Kip1 tumor suppression and MAPK activation in a tissue-specific manner. Oncogene 24:1718–1726, 2005.
8. Trosko JE, Ruch RJ. Cell-cell communication in carcinogenesis. Front Biosci 3:D208–D236, 1998.
9. Temme A, Buchmann A, Gabriel HD, Nelles E, Schwarz M, Willecke K. High incidence of spontaneous and chemically induced liver tumors in mice deficient for connexin32. Curr Biol 7:713–716, 1997.
10. Jeong SH, Habeebu SS, Klaassen CD. Cadmium decreases gap junctional intercellular communication in mouse liver. Toxicol Sci 57:156–166, 2000.
11. Rosendaal M, Gregan A, Green CR. Direct cell-cell communication in the blood-forming system. Tissue Cell 23:457–470, 1991.
12. Ploemacher RE, Mayen AE, De Koning AE, Krenacs T, Rosendaal M. Hematopoiesis: gap junction intercellular communication is likely to be involved in regulation of stroma-dependent proliferation of hemopoietic stem cells. Hematology 5:133–147, 2000.
13. Cancelas JA, Koevoet WL, de Koning AE, Mayen AE, Rombouts EJ, Ploemacher RE. Connexin-43 gap junctions are involved in multiconnexin-expressing stromal support of hemopoietic progenitors and stem cells. Blood 96:498–505, 2000.
14. Montecino-Rodriguez E, Leathers H, Dorshkind K. Expression of connexin 43 (Cx43) is critical for normal hematopoiesis. Blood 96: 917–924, 2000.
15. Yoon BI, Hirabayashi Y, Kawasaki Y, Tsuboi I, Ott T, Kodama Y, Kanno J, Kim DY, Willecke K, Inoue T. Exacerbation of benzene pneumotoxicity in connexin 32 knockout mice: enhanced proliferation of CYP2E1-immunoreactive alveolar epithelial cells. Toxicology 195: 19–29, 2004.
16. Krenacs T, Rosendaal M. Connexin43 gap junctions in normal, regenerating, and cultured mouse bone marrow and in human

leukemias: their possible involvement in blood formation. Am J Pathol 152:993–1004, 1998.
17. Keller JR, Mantel C, Sing GK, Ellingsworth LR, Ruscetti SK, Ruscetti FW. Transforming growth factor beta 1 selectively regulates early murine hematopoietic progenitors and inhibits the growth of IL-3-dependent myeloid leukemia cell lines. J Exp Med 168:737–750, 1988.
18. Sasaki H, Matsuda M, Lu Y, Ikuta K, Matsuyama S, Hirabayashi Y, Mitsui H, Matsumura T, Muramatsu M, Tsukada T, Aizawa S, Inoue T. A fraction unresponsive to growth inhibition by TGF-beta among the high-proliferative potential progenitor cells in bone marrow of p53-deficient mice. Leukemia 11:239–244, 1997.
19. Nelles E, Butzler C, Jung D, Temme A, Gabriel HD, Dahl U, Traub O, Stumpel F, Jungermann K, Zielasek J, Toyka KV, Dermietzel R, Willecke K. Defective propagation of signals generated by sympathetic nerve stimulation in the liver of connexin32-deficient mice. Proc Natl Acad Sci U S A 93:9565–9570, 1996.
20. Yoon BI, Hirabayashi Y, Kawasaki Y, Kodama Y, Kaneko T, Kim DY, Inoue T. Mechanism of action of benzene toxicity: cell cycle suppression in hemopoietic progenitor cells (CFU-GM). Exp Hematol 29:278–285, 2001.
21. Sander B, Andersson J, Andersson U. Assessment of cytokines by immunofluorescence and the paraformaldehyde-saponin procedure. Immunol Rev 119:65–93, 1991.
22. Hirabayashi Y, Inoue T, Suda Y, Aizawa S, Ikawa Y, Kanisawa M. Hemopoietic neoplasms in lethally irradiated mice repopulated with bone marrow cells carrying the human c-myc oncogene: a repopulation assay. Exp Hematol 20:167–172, 1992.
23. Till JE, McCulloch EA. A direct measurement of the radiation sensitivity of normal mouse bone marrow cells. Radiat Res 14:213–222, 1961.
24. Hirabayashi Y, Matsuda M, Aizawa S, Kodama Y, Kanno J, Inoue T. Serial transplantation of p53-deficient hemopoietic progenitor cells to assess their infinite growth potential. Exp Biol Med (Maywood) 227: 474–479, 2002.
25. Inoue T, Cronkite EP, Commerford SL, Carsten AL. Residual toxicity in hematopoietic cells following a single dose of methylnitrosourea. Leuk Res 8:105–116, 1984.
26. Hirabayashi Y, Yoshida K, Aizawa S, Kodama Y, Kanno J, Kurokawa Y, Yoshimura I, Inoue T. Evaluation of nonthreshold leukemogenic response to methyl nitrosourea in p53-deficient C3H/He mice. Toxicol Appl Pharmacol 190:251–261, 2003.
27. Hirabayashi Y, Inoue T, Yoshida K, Inayama Y, Kanisawa M. The detection of normal hidden stem cells during the development of leukemia: assays with PGK isozyme. Exp Hematol 18:7–10, 1990.
28. Tanaka T, Suda T, Suda J, Inoue T, Hirabayashi Y, Hirai H, Takaku F, Miura Y. Stimulatory effects of granulocyte colony-stimulating factor on colony-forming units-spleen (CFU-S) differentiation and pre-CFU-S proliferation in mice. Blood 77:2597–2602, 1991.
29. Magli MC, Iscove NN, Odartchenko N. Transient nature of early haematopoietic spleen colonies. Nature 295:527–529, 1982.
30. Shibagaki T, Inoue T, Kubota N, Kanisawa M. Fraction of pluripotent hemopoietic stem cells in DNA synthesis varies with generation age. Exp Hematol 14:794–797, 1986.
31. Rosendaal M, Hodgson GS, Bradley TR. Organization of haemopoietic stem cells: the generation-age hypothesis. Cell Tissue Kinet 12:17–29, 1979.
32. Ogawa M, Bergsagel DE, McCulloch EA. Sensitivity of human and murine hemopoietic precursor cells to chemotherapeutic agents assessed in cell culture. Blood 42:851–856, 1973.
33. Campbell FR. Gap junctions between cells of bone marrow: an ultrastructural study using tannic acid. Anat Rec 196:101–107, 1980.
34. Campbell FR. Intercellular contacts between migrating blood cells and cells of the sinusoidal wall of bone marrow. An ultrastructural study using tannic acid. Anat Rec 203:365–374, 1982.
35. King TJ, Lampe PD. Mice deficient for the gap junction protein Connexin32 exhibit increased radiation-induced tumorigenesis associated with elevated mitogen-activated protein kinase (p44/Erk1, p42/Erk2) activation. Carcinogenesis 25:669–680, 2004.
36. King TJ, Lampe PD. The gap junction protein connexin32 is a mouse lung tumor suppressor. Cancer Res 64:7191–7196, 2004.

Inflammatory Biomarker, Neopterin, Suppresses B Lymphopoiesis for Possible Facilitation of Granulocyte Responses, Which Is Severely Altered in Age-Related Stromal-Cell–Impaired Mice, SCI/SAM

AKIHIRO MINAMI,* ISAO TSUBOI,*,[1] TOMONORI HARADA,* TOSHITAKA FUKUMOTO,* MASAKI HIRAMOTO,* MORIMICHI KOSHINAGA,* YOKO HIRABAYASHI,† JUN KANNO,† TOHRU INOUE,‡ AND SHIN AIZAWA*

*Department of Anatomy, Nihon University School of Medicine, Tokyo 173-8610, Japan; †Division of Cellular and Molecular Toxicology, Center for Biological Safety and Research, National Institute of Health Science, Tokyo 158-8501, Japan; and ‡Center for Biological Safety and Research, National Institute of Health Science, Tokyo 158-8501, Japan

Neopterin is produced by monocytes and is a useful biomarker of inflammatory activation. We found that neopterin enhanced *in vivo* and *in vitro* granulopoiesis triggered by the stromal-cell production of cytokines in mice. The effects of neopterin on B lymphopoiesis during the enhancement of granulopoiesis were determined using the mouse model of senescent stromal-cell impairment (SCI), a subline of senescence-accelerated mice (SAM). In non-SCI mice (a less senescent stage of SCI mice), treatment with neopterin decreased the number of colonies, on a semisolid medium, of colony-forming units of pre–B-cell progenitors (CFU-preB) from unfractionated bone marrow (BM) cells, but not that from a population rich in pro-B and pre-B cells without stromal cells. Neopterin upregulated the expression of genes for the negative regulators of B lymphopoiesis such as tumor necrosis factor-α (TNF-α), interleukin-6 (IL-6), and transforming growth factor-β (TGF-β) in cultured stromal cells, implying that neopterin suppressed the CFU-preB colony formation by inducing negative regulators from stromal cells. The intraperitoneal injection of neopterin into non-SCI mice resulted in a marked decrease in the number of femoral CFU-preB within 1 day, along with increases in TNF-α and IL-6 expression levels. However, in SCI mice, *in vivo* and *in vitro* responses to B lymphopoiesis and the upregulation of cytokines after neopterin treatment were less marked than those in non-SCI mice. These results suggest that neopterin predominantly suppressed lymphopoiesis by inducing the production of negative regulators of B lymphopoiesis by stromal cells, resulting in the selective suppression of *in vivo* B lymphopoiesis. These results also suggest that neopterin facilitated granulopoiesis in BM by suppressing B lymphopoiesis, thereby contributing to the potentiation of the inflammatory process; interestingly, such neopterin function became impaired during senescence because of attenuated stromal-cell function, resulting in the downmodulation of the host-defense mechanism in the aged. Exp Biol Med 232:134–145, 2007

Key words: neopterin; B lymphopoiesis; stromal-cell–impaired mouse; subline of senescence-accelerated mice; aging

Introduction

Neopterin is a metabolite of guanosine triphosphate that is produced in the biopterin synthetic pathway (1). *In vitro,* large amounts of this metabolite are generated by "monocytes and macrophages" in response to interferon-γ (IFN-γ) (2). Because increased neopterin levels accompany immune responses *in vivo* and *in vitro,* there has been considerable interest in measuring neopterin levels as a biomarker of immunologic activation (2–4).

The possible immunologic relevance of neopterin pertinent to inflammatory processes has been considered on the basis of observations that neopterin induces apoptosis in rat alveolar epithelial cells L2 (5) and inhibits NADPH-oxidase in peritoneal macrophages (6). Moreover, neopterin has been found to inhibit erythropoietin gene expression (7)

This work was supported in part by a grant from the Ministry of Education, Culture, Sports, Science, and Technology of Japan for the promotion of industry-university collaboration at Nihon University and also by a Nihon University Joint Research Grant for 2004.

[1] To whom correspondence should be addressed at Department of Anatomy, Nihon University School of Medicine, 30–1 Ohyaguchi-kamimachi, Itabashiku, Tokyo 173-8610, Japan. E-mail: tsuboi@med.nihon-u.ac.jp

Received January 29, 2006.
Accepted May 26, 2006.

1535-3702/07/2321-0134$15.00

and induce the expression of genes for proto-oncogene c-*fos* (8) and nitric oxide synthase (9). Furthermore, because the gene expression of the gene for inducible nitric oxide synthase (iNOS) and the subsequent nitric oxide (NO) release from vascular smooth muscle cells (VSMCs) following incubation with neopterin have been documented, neopterin is supposed to play a role as a modulator in gram-negative endotoxemia that contributes to the excessive production of NO (9, 10).

Neopterin, on the other hand, increases the number of colony-forming units of granulocyte-macrophage progenitor cells (CFU-GM) in a semisolid culture system (11), and intraperitoneal neopterin injection into mice stimulates granulopoiesis (12). This stimulation of *in vitro* and *in vivo* granulopoiesis is due not to a direct action of neopterin on hematopoietic stem cells, but rather to an indirect effect mediated by the stromal-cell production of hematopoietic growth factors, such as granulocyte-macrophage colony-stimulating factor and interleukin-6 (IL-6) (11). Thus, regarding the most interesting characteristics of neopterin, we would like to clarify how this biosynthetic compound functions not only in immune responses but also in hematopoietic anti-inflammatory responses.

To answer the above question, SAM/P-1, a subline of senescence-accelerated mice (SAM) exhibiting a unique stromal-cell impairment after 30 weeks of age, was used, because in SAM the numbers of splenic cells and splenic hematopoietic progenitor cells start to decrease (13–15). Furthermore, senescent SAM/P-1 mice show the simultaneous downregulations of interleukin-7 (IL-7) and transforming growth factor-β (TGF-β) caused by the suppression of B lymphopoiesis in senescence (16). Interestingly, the murine system possesses a markedly low level of neopterin in the circulation in the steady state; thus, the SAM/P-1 mouse model may be a useful tool for elucidating the possible interaction of neopterin and stromal cells during B lymphopoiesis. Thus, we investigated whether neopterin affects B lymphopoiesis using stromal-cell–impaired (SCI) mice, a subline of SAM/P-1 mice.

In this study, we suggest the functions of neopterin in the mechanisms underlying the suppression of B lymphopoiesis, consequent facilitation of potentiation of granulopoiesis, and further functional impairment during senescence.

Materials and Methods

Mice. A subline of SAM, SAM/P-1 (13), is a senescent stromal-cell impairment substrain (SCI mice), derived from AKR mice (Jackson Laboratory, Bar Harbor, ME), and established by Dr. Toshio Takeda, Professor Emeritus of the Chest Disease Research Institute, Kyoto University, Japan. The mice were bred and maintained in an experimental facility at the National Institute of Health Sciences under pathogen-free conditions. SAM/P-1 exhibits stromal-cell impairment after 30 to 36 weeks of age. In this study, male SAM/P-1 mice designated as non-SCI mice (8 to 12 weeks old) and SCI mice (30 to 36 weeks old) were compared. These ages were selected because the numbers of splenic cells and splenic hematopoietic progenitor cells start to decrease significantly at approximately 30 weeks of age (15, 16). The study was approved by the Institutional Animal Care and Use Committee at the National Institute of Health Science guidelines for animal care.

Neopterin. D(+) neopterin was obtained from Sigma (St. Louis, MO). Neopterin was dissolved in 1 *N* HCl at 1 mg/ml and diluted tenfold with Dulbecco's phosphate-buffered saline (PBS).

Neopterin Administration. The mice were injected intraperitoneally with neopterin (0.35 or 3.5 mg/kg body weight) for single-dose administration or on three consecutive days. The doses chosen here correspond to those for humans determined in the laboratory; however, the doses chosen are highly biased because the steady-state background dose of neopterin in rodents, in general, is significantly lower than those in humans and nonhuman primates; that is, lower than one n*M* per liter (12,925 and 85 n*M*, 30 and 60 mins, respectively, after 3.5 mg/kg body weight neopterin administered). The mice were evaluated, in the case of a single dose, 0.5, 1, 2, 3, 6, and 24 hrs after the administration, and, in the case of three doses, 1, 7, and 14 days after the last injection. As the control, a group of mice was injected with the same volume of PBS with the same amount of HCl as that used as the vehicle for neopterin. Three mice per group were examined for each data point.

Bone Marrow (BM) Cells. BM cells were isolated by repeatedly flushing cells from femurs using Iscove-modified Dulbecco's medium (IMDM; Invitrogen, Carlsbad, CA) or RPMI 1640 medium (Invitrogen). The BM cells were suspended by trituration using a 23-gauge hypodermic needle.

Preparation of Pro–B/Pre–B-Cell–Rich Populations. To obtain populations rich in pro-B cells and pre-B cells without stromal-cell components, the bulk culture of pooled BM cells from the non-SCI and SCI mice was stimulated with recombinant interleukin-7 (rIL-7) as described previously (16, 17). Briefly, BM cells were cultured at 1×10^6 cells/ml in RPMI 1640 supplemented with 20% fetal bovine serum (FBS; Hyclone Laboratories Inc., Logan, UT), 20 μ*M* 2-mercaptoethanol, 1% L-glutamine, and 2 ng/ml murine rIL-7 (Genzyme, Cambridge, MA) in six-well tissue culture plates (Falcon 3046; Beckton-Dickinson, Franklin Lake, NJ). Nonadherent cells were harvested after 4 days. This bulk culture provides a 10 times richer source of IL-7–responsive $B220^+/CD43^+/IgM^-$ pro-B/pre-B cells (16), which provide a functionally homogeneous large number of fractions requiring only gentler and easier detachment of B lymphocytes from stromal cells.

***In Vitro* Colony Assays.** Colony formation by colony-forming-unit pre-B cells (CFU-preB cells) was assayed using a semisolid medium containing rIL-7 (16).

Femoral BM cells from three mice per group were pooled and assayed in 35-mm plastic Petri dishes containing 1 ml of MethoCult M 3630 medium (Stem Cell Technologies Inc., Vancouver, Canada), which consisted of IMDM composed of 1% methylcellulose, supplemented with 30% FBS, 0.1 m*M* 2-mercaptoethanol, 2 m*M* L-glutamine, and 10 ng/ml rIL-7. Triplicate culture plates containing equal amounts of CFU-preB cells estimated were incubated at 37°C in a fully humidified atmosphere of 5% CO_2 in air. After 7 days, aggregates of 50 or more cells were counted as colonies.

Preparation of Cultured Stromal Cells. Stromal-cell monolayers were prepared by culturing whole BM cells derived from non-SCI or SCI mice at 1×10^6/ml cells in 10-cm diameter cell culture dishes (Corning Incorporated, Corning, NY) or 24-well flat bottom plates (Falcon 3047) in 30 ml or 1 ml of IMDM supplemented with 10% FBS. Confluent adherent layers were formed after 10 days of culture. The supernatant was removed and cultured dishes with confluent adherent layer were rinsed with IMDM twice to eliminate nonadherent cells. A fresh culture medium containing 4 μ*M* or 400 n*M* neopterin was then added to 10-cm diameter cell culture dishes or 24-well flat bottom plates, and the cells were further incubated. As for 10-cm diameter cell culture dishes, after 1, 3, and 9 hrs of incubation, the culture medium was removed completely and stromal cells were subjected to RNA extraction. As for 24-well flat bottom plates, after 24 hrs of incubation, the culture medium was collected and was used for determination of the levels of tumor necrosis factor-α (TNF-α), IL-6, and TGF-β proteins produced by cultured stromal cells. The concentration of TNF-α, IL-6, or TGF-β in the culture medium was determined using TNF-α, IL-6, or TGF-β–specific enzyme-linked immunosorbent assay (ELISA) kit (R&D Systems, Minneapolis, MN) according manufacturer's instructions. All the samples were assayed in triplicate.

Total RNA Extraction and Quantitative Real-Time Polymerase Chain Reaction (PCR). Total RNA was extracted from BM cells using TRIzol (Invitrogen) according to the manufacturer's instructions. The isolated mRNA was reverse transcribed using Superscript (Life Technologies, Grand Island, NY) and Oligo-dT (Promega, Madison, WI). Next, quantitative real-time PCR was performed using a TaqMan Universal PCR master mix (Applied Biosystems, Foster City, CA) and specific primers and probes, with the Applied Biosystems 7900 sequence detection system, version 2.0. Specific primers and probes for murine IL-7, TNF-α, IL-6, TGF-β, and glyceraldehyde phosphate dehydrogenase (GAPDH) were purchased from Applied Biosystems (TaqMan Gene Expression Assays; IL-7, Mm00434291_m1; TNF-α, Mm00443281_m1; IL-6, Mm 00446190_m1; TGF-β, Mm00441724 _m1; GAPDH, Mm99999915_g1). PCR conditions and data analysis were performed according to the instructions in the Sequence Detection System, version 2.0. In this study, total RNA extraction and expression of GAPDH were compared between non-SCI and SCI mice (data are shown in Appendix). All reactions were performed in triplicate. According to the manufacturer's instructions, cytokine-specific signals were normalized by the GAPDH signal using the formula $2^{-\Delta Ct} = 2^{-[Ct(GAPDH) - Ct(cytokine)]}$, and the relative level of cytokine gene expression was calculated using $2^{-\Delta\Delta Ct} = 2^{-(\Delta Ct \text{ for neopterin treatment} - \Delta Ct \text{ for control})}$, where Ct is the threshold cycle.

Statistical Analyses. Data were subjected to analysis of variance (ANOVA). Values were considered significantly different at $P < 0.05$.

Results

Effects of Neopterin on *in Vitro* CFU-PreB Colony Formation from Unfractionated BM Cells and Populations Rich in Pro-B/Pre-B Cells: Comparison Between Non-SCI and SCI. To determine whether neopterin directly affects the proliferation or differentiation of pre–B-cell progenitors, we cultured whole (unfractionated) BM cells from non-SCI and SCI mice in a semisolid medium system containing rIL-7 and in the presence of various concentrations of neopterin and measured the number of colonies formed (Fig. 1). In the colonization assays without neopterin, the absolute numbers of colonies from the non-SCI and SCI mice were significantly different, that is 137 ± 10 and 37 ± 1 per 2×10^5 cells, respectively. In Figure 1, each value is expressed as 100% of control, revealing the *in vitro* effects of neopterin on CFU-preB colonies in whole BM cells from non-SCI and SCI mice. When graded increasing doses of neopterin from 4 n*M* to 4 μ*M* were administered, the number of CFU-preB colonies from non-SCI BM cells decreased in a dose-dependent manner compared with that of the nontreated control groups, and except for the lowest dose at 4 n*M*, the other three higher dose groups all showed statistically significant decreases (10.5%, 24.2%, 26.9%, and 35.7% for 4 n*M*, 40 n*M**, 400 n*M**, and 4 μ*M**, respectively; *$P < 0.05$). Interestingly, these decreases in the number of CFU-preB colonies were observed to be smaller in those from senescent SCI BM cells. Namely, there were no significant decreases observed in the number of CFU-preB cells from SCI BM cells except at the highest dose of 4 μ*M* (0%, 5.0% , 17.2%, and 28.5%, for 4 n*M*, 40 n*M*, 400 n*M*, and 4 μ*M* [$P < 0.05$], respectively); thus, it may be concluded that the groups treated with neopterin at the three lower concentrations did not show the suppression of B-cell colonization of BM cells in the senescent SCI groups as compared with those of the young non-SCI groups. When the reduction ratios at the same dose of neopterin treated groups were compared between non-SCI and SCI, a statistically significant difference was observed for solely the dose at 40 n*M* ($P < 0.05$).

However, the above suppression of CFU-preB colony formation was not observed when BM cells were cultured, under IL-7 stimulation, with the population rich in pro-B and pre-B cells isolated and seeded prior to neopterin

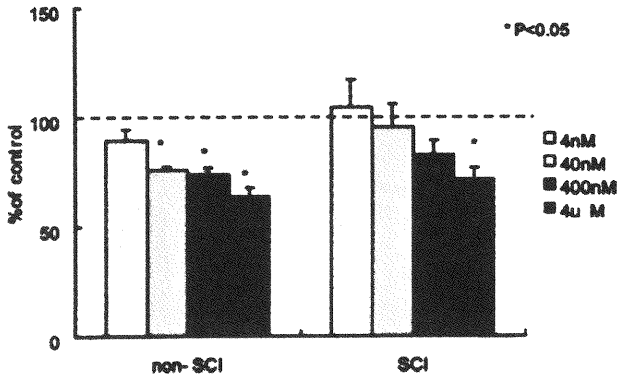

Figure 1. CFU-preB colony formation of whole BM cells from non-SCI and SCI mice in the presence of neopterin. Unfractionated BM cells from the non-SCI and SCI mice were incubated in a semisolid culture system containing interleukin-7 (IL-7) in the presence or absence of neopterin. The number of colonies was determined after 7 days. The absolute numbers of colonies in cultures without neopterin for the non-SCI and SCI mice were significantly different (137 ± 10 and 37 ± 1 per 2×10^5 cells, respectively; $P < 0.001$; data not shown). The reduction ratios following neopterin treatment are expressed as percentage relative to the nontreated control of each group, namely, non-SCI and SCI mice. Each bar represents the mean ± standard deviation (SD) from triplicate experiments (*$P <$ 0.05 vs. each control). The comparison of reduction ratios between non-SCI and SCI showed statistical significance only at the lowest dose, that is 40 n*M* ($P < 0.05$).

treatment regardless of the use of non-SCI and SCI mouse BM cells (data not shown). Thus, the above data imply that the suppression of the colonization of CFU-preB progenitor cells by neopterin treatment is presumably due to a stromal-cell–mediated effect.

Gene Expressions and Protein Productions of TNF-α, IL-6, and TGF-β in Cultured Stromal Cells Induced by Neopterin: Comparison Between Non-SCI and SCI. To elucidate the mechanism underlying the suppression of CFU-preB-cell progenitor colony formation, which is presumably induced by stromal cells, messenger RNAs of principal cytokine genes for the negative regulation of the pro-B/pre-B fraction were evaluated, namely, TNF-α, IL-6, and TGF-β. Figure 2 shows the time course of cytokine gene expression levels in stromal cells cultured in the presence of 4 μ*M* neopterin. The results were expressed as a ratio to each cultured non-SCI or SCI fraction without neopterin. In non-SCI stromal cells (Fig. 2A–C), neopterin transiently and modestly suppressed the expressions of TNF-α, IL-6, and TGF-β genes from 1 to 3 hrs and then continuously upregulated the gene expressions until 9 hrs. The gene expression levels of TNF-α, IL-6, and TGF-β in cultured stromal cells 9 hrs after neopterin treatment increased by 1.63-, 1.93- and 2.07-fold (asterisks), respectively, compared with those in the control stromal cells without neopterin treatment ($P < 0.001$). In contrast to non-SCI cultured stromal cells, neopterin did not increase the gene expression levels of TNF-α, IL-6, and TGF-β in cultured SCI cells compared with those in SCI cells without neopterin treatment (Fig. 2D–F). Therefore, it is clear that the gene expression levels of TNF-α, IL-6, and TGF-β in cultured SCI cells and non-SCI cells show significant differences (A vs. D, $P < 0.001$; B vs. E, $P < 0.005$; and C vs. F, $P < 0.001$, respectively). After 24 hrs commercially available ELISA kits showed essentially comparable data, although 400 n*M* neopterin elicited much higher responses (23 ± 3 to 76 ± 11 pg/ml [$P < 0.05$] for non-SCI and 22 ± 8 to 38 ± 8 pg/ml for SCI, nontreated with 400 n*M* for TNF-α; 191 ± 25 to 455 ± 92 pg/ml [$P < 0.05$] for non-SCI and 155 ± 14 to 184 ± 11 pg/ml for SCI, nontreated with 400 n*M* for IL-6; 220 ± 15 to 298 ± 28 pg/ml [$P <$ 0.05] for non-SCI and 68 ± 24 to 115 ± 43 pg/ml for SCI, nontreated with 400 n*M* for TGF-β; Table 1).

Neopterin-Induced B-Lymphopoietic Regulation in BM *in Vivo*: Comparison Between Non-SCI and SCI. Neopterin at doses 0.35 mg/kg body weight and 3.5 mg/kg body weight was intraperitoneally injected into non-SCI mice and SCI mice, respectively, to determine the stromal effect of neopterin on B lymphopoiesis (data not shown). The absolute numbers of CFU-preB progenitor cells observed in the femur of non-SCI mice and SCI mice were 9438 ± 177 and 3140 ± 57, respectively. As expected, on Day 1 after the three doses of daily treatment with neopterin, significant decreases in the number of CFU-preB progenitor cells in the femoral BM were observed in both non-SCI mice and SCI mice (43.1% [$P < 0.001$] and 22.9% [$P < 0.001$] for non-SCI mice, whereas 82.9% [$P >$ 0.05] and 45.1% [$P < 0.005$] for SCI mice; relative to those of the control at 0.35 mg/kg body weight and 3.5 mg/kg body weight, respectively); thus, the suppression was markedly milder in the senescent SCI mice than in the non-SCI mice. To determine the effects of neopterin at the *in vivo* level, the same three daily treatments at 3.5 mg/kg body weight were carried out on both non-SCI mice and SCI mice, and the number of femoral CFU-preB progenitor cells was evaluated 1, 7, and 14 days after the last treatment with neopterin. As observed in Figure 3, the number of femoral CFU-preB progenitor cells shows a prominent oscillation, that is, a statistically significant decrease in number on Day 1 (22.9% of that from the nontreated non-SCI mice), followed by a marked increase on Day 7 (209% that from the nontreated non-SCI), and then returns to the nontreated control level of the non-SCI mice. Very interestingly, not only the number of CFU-preB progenitor cells in the nontreated group but also the oscillatory extent was smaller in the SCI mice. In this figure, the marked overshoot increase in the number of CFU-preB progenitor cells from the SCI mice is smaller than that from the nontreated non-SCI mice (number in nontreated non-SCI mice, 9438 ± 177 vs. number on Day 7 in treated SCI mice, 5134 ± 292).

Gene Expressions of IL-7, TNF-α, IL-6, and TGF-β in BM *in Vivo* During Neopterin-Induced Pre–B-Cell Suppression: Comparison Between Non-SCI and SCI. To elucidate the mechanism underlying the oscillation presumably induced by stromal cells, the

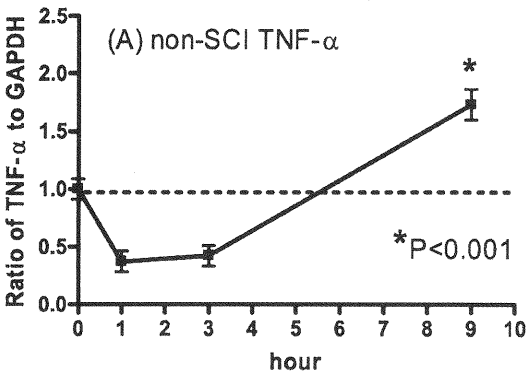
(A) non-SCI TNF-α
Ratio of TNF-α to GAPDH
*P<0.001
hour

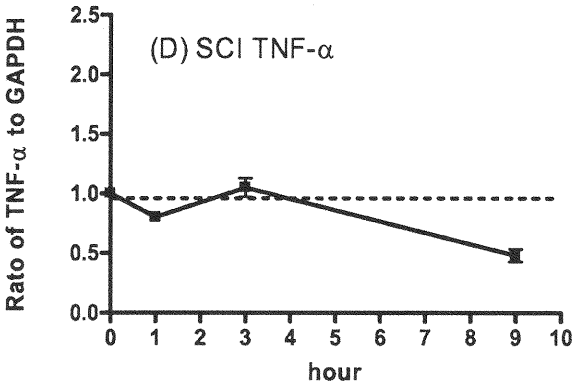
(D) SCI TNF-α
Rato of TNF-α to GAPDH
hour

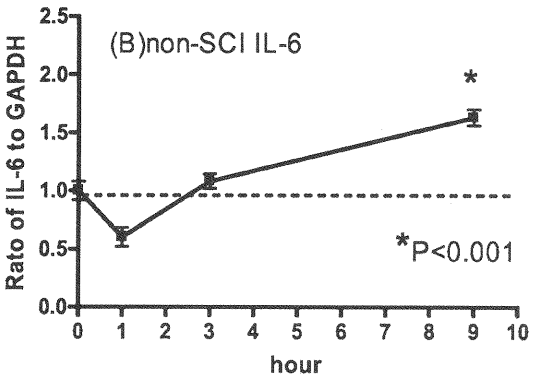
(B)non-SCI IL-6
Rato of IL-6 to GAPDH
*P<0.001
hour

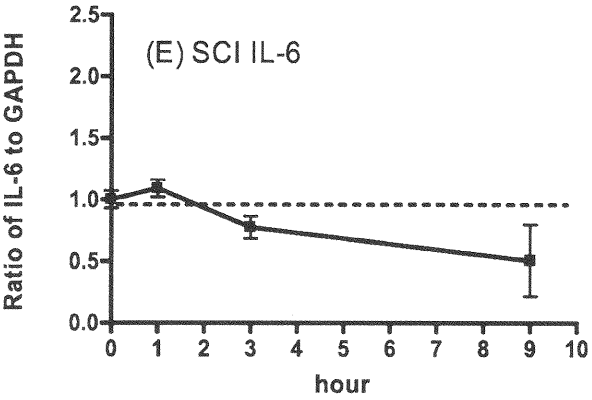
(E) SCI IL-6
Ratio of IL-6 to GAPDH
hour

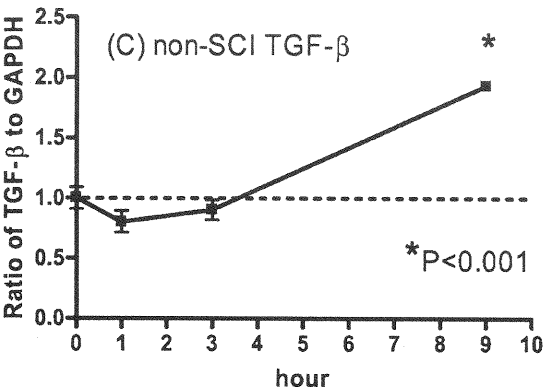
(C) non-SCI TGF-β
Ratio of TGF-β to GAPDH
*P<0.001
hour

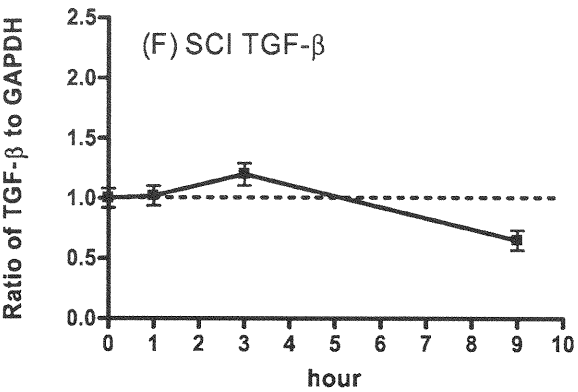
(F) SCI TGF-β
Ratio of TGF-β to GAPDH
hour

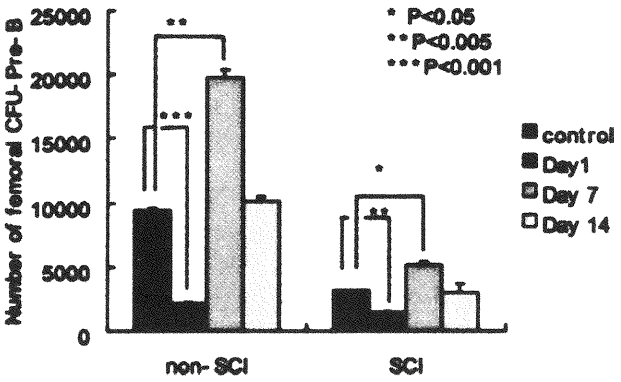

Figure 3. Time courses of numbers of CFU-preB in BM cells from non-SCI and SCI mice after neopterin treatment. Femoral BM samples of the non-SCI and SCI mice were obtained from three non-SCI mice and SCI mice 1, 7, and 14 days after the intraperitoneal injection of neopterin (3.5 mg/kg) for three consecutive days. The changes in the number of CFU-preB cells were determined. Each bar represents the mean ± SD obtained from triplicate experiments. $^*P < 0.05$, $^{**}P < 0.005$,$^{***}P < 0.001$ vs. each control.

messenger RNAs of principal cytokine genes for the positive and negative regulations of the pro-B/pre-B fraction were evaluated, namely, IL-7, TNF-α, IL-6, and TGF-β. In Figure 4, the short-term effects of neopterin on cytokine gene expression levels in BM cells were evaluated 30 min and 1, 2, 3, 6, and 24 hrs after the single-dose neopterin administration because the half-life of neopterin is 90 min (18). In each panel, the results are expressed as a treatment normalized by GAPDH expression level, respectively. Absolute GAPDH expression levels in non-SCI or SCI mice did not show significant differences from each other (see Appendix). In the non-SCI mice, the gene expression levels of the negative regulators TNF-α and IL-6 increased markedly up to sixfold at 1 hr followed by a mild increase up to 6 hrs, although that of TGF-β showed an increase throughout, although not significant. During the course of the experiment, the positive regulator IL-7 showed a very mild increase from 3 to 6 hrs. Regardless of being positive and negative regulators, the expression levels of IL-7, TNF-α, IL-6, and TGF-β all decreased or came back to the level of nontreated control by 24 hrs. In the SCI mice, the negative regulator TNF-α, IL-6, or TGF-β was not expressed at all, except that a milder and delayed peak was observed for IL-6 at 2 hrs. The positive regulator IL-7 showed a milder increase in the same manner as that in non-SCI mice from 3 to 6 hrs. The suppression of cytokine gene expression in the SCI mice at 24 hrs was not observed for all the positive and negative regulators; specifically for TGF-β, the expression levels were slightly higher than those in the nontreated control SCI mice (44.0%, 28.0%, 43.6%, and 92.4%, vs. 128.5%, 130.0%, 274.6%, and 138.5%, for IL-7, TNF-α, IL-6, and TGF-β, respectively).

Table 1. Concentrations of Cytokines in the Supernatant of Cultured Stromal Cells from Non-SCI and SCI Mice[a]

Concentration of neopterin	Non-SCI		SCI	
	None	400 n*M*	None	400 n*M*
TNF-α pg/ml)	23 ± 3	76 ± 11*	22 ± 8	38 ± 8
IL-6 pg/ml)	191 ± 25	455 ± 92*	155 ± 14	184 ± 11
TGF-β pg/ml)	220 ± 15	298 ± 28*	68 ± 24	115 ± 43

[a] Supernatant of cultured stromal cells was collected 24 hrs after treatment with 400 n*M* neopterin, and concentrations of cytokines in the supernatant was measured by ELISA methods. Each data point represents the mean ± SD obtained from triplicate experiments. $^*P < 0.05$ vs. each control.

When neopterin was administered for 3 days, the prolonged effect of neopterins on cytokine gene expression was evaluated only 1 and 7 days after the treatment (Fig. 5). Again, the degrees of suppression of the genes expressions of IL-7, TNF-α, IL-6, and TGF-β on Day 1 in the non-SCI mice were 0.56, 0.78, 0.51, and 0.32 relative to those in the nontreated non-SCI mice considered as 1.0, respectively. All the gene expression levels returned to the control level on Day 7. Interestingly, again, the relative changes in these cytokine gene expressions in the SCI mice were essentially milder than those in the non-SCI mice except for IL-7 (0.47, 0.96, 0.81, and 0.84, relative to those of the nontreated SCI control considered as 1.0; senescent SCI mice for IL-7, TNF-α, IL-6, and TGF-β, respectively).

A significant decrease in the number of CFU-preB progenitor cells shown in Figures 4 and 5 may be supported by data shown in Figure 6, in which the steady-state contributions of the positive regulator IL-7 and the negative regulators TNF-α, IL-6, and TGF-β are shown with respect to their absolute expression levels relative to each of the non-SCI and SCI gene expression levels of GAPDH in each of the non-SCI and SCI control. As observed from the absolute cytokine level, the expressions of TGF-β and IL-6

←

Figure 2. Time courses of TNF-α, IL-6, and TGF-β gene expression levels in stromal cells from young non-SCI and elderly SCI mice (A, B, C and D, E, F, respectively) cultured in the presence of neopterin. Stromal monolayers were prepared by culturing unfractionated BM cells derived from non-SCI or SCI mice. The supernatant was removed and the culture dishes with confluent adherent layer were rinsed with IMDM twice to eliminate nonadherent cells. A fresh culture medium containing 4 μ*M* neopterin was then added and the cells were incubated further. After 1, 3, and 9 hrs of incubation, the culture medium was removed completely and stromal cells were subjected to RNA extraction. Total RNA was extracted from the cultured stromal cells of the non-SCI and SCI mice with TRIzol (Invitrogen) according to the manufacturer's instructions. The reverse-transcribed complementary DNAs were amplified by real-time reverse transcription–polymerase chain reaction (real-time RT-PCR) using the TaqMan universal PCR master mix (Applied Biosystems) and specific primers for murine TNF-α, IL-6, TGF-β, and GAPDH. GAPDH gene expression levels are the same in non-SCI and SCI mice (see Appendix). The results are expressed as a ratio to the cultured non-SCI or SCI fraction without neopterin. Each bar represents the mean ± SD obtained from triplicate experiments ($^*P < 0.001$ vs. each control).

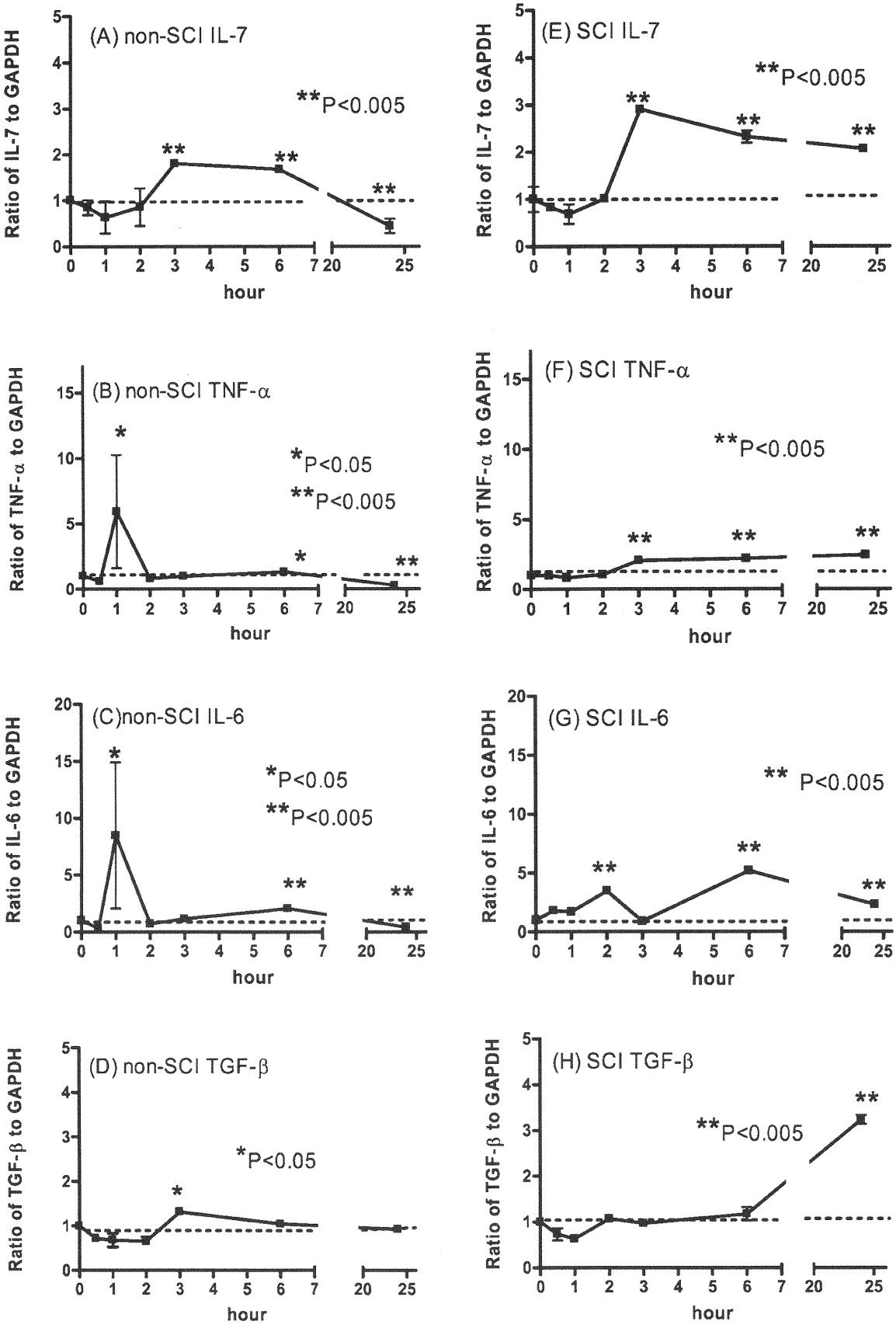
(A) non-SCI IL-7
**P<0.005
Ratio of IL-7 to GAPDH
hour
(E) SCI IL-7
**P<0.005
Ratio of IL-7 to GAPDH
hour
(B) non-SCI TNF-α
*P<0.05
**P<0.005
Ratio of TNF-α to GAPDH
hour
(F) SCI TNF-α
**P<0.005
Ratio of TNF-α to GAPDH
hour
(C)non-SCI IL-6
*P<0.05
**P<0.005
Ratio of IL-6 to GAPDH
hour
(G) SCI IL-6
** P<0.005
Ratio of IL-6 to GAPDH
hour
(D) non-SCI TGF-β
*P<0.05
Ratio of TGF-β to GAPDH
hour
(H) SCI TGF-β
**P<0.005
Ratio of TGF-β to GAPDH
hour

markedly predominate as compared with that of IL-7 (43.2, 60.3, and 657.5 relative to expression level IL-7 from nontreated non-SCI mice considered as 1.0, nontreated non-SCI mice for TNF-α, IL-6, and TGF-β, respectively).

Discussion

Neopterin, a guanosine derivative, is an inflammatory byproduct that stimulates the proliferation of granulocytes and their progenitor cells due to stromal-cell–derived cytokines, such as GM-CSF and IL-6 (11, 12). During the inflammatory process, the production of lymphocytes is occasionally suppressed when granulocyte proliferation is stimulated (19–21). Thus, whether lymphocyte proliferation is stimulated or suppressed by the inflammatory byproduct neopterin, during the suppurative inflammatory process is of interest. During the suppurative inflammatory process, T cells undergo apoptosis induced by 7,8-dehydroneopterin (22). Thus, in this study, we attempted to clarify the effect of neopterin on the B-cell lineage to determine whether such a suppressive mechanism also exists in this lineage.

We conducted the experiment with the aim of determining the possible regulatory mechanism of inflammatory cytokines in the B-cell lineage. It should be noted that because the basal level of neopterin in rodents was lower than that in primates, including humans, the dose of neopterin used in the present study was markedly lower than those used in previous studies (5, 7, 9, 23, 24), and neopterin was still clearly detectable. Interestingly, when the B-cell lineage was treated with neopterin to determine whether B-cell suppression might occur, the suppressive effect was induced, presumably by different cytokines specific to B-cell lineages released from stromal cells as in the case of granulopoiesis observed previously (11, 12). Furthermore, we found that this suppressive effect was milder when stromal cells were derived from SCI mice, although this significant mildness in SCI mice compared with those in non-SCI mice was not always significant in terms of relative suppressive ratios between non-SCI and SCI, which was only significant at the dose of 40 n*M*. SAM/P-1 mice used in the experiment showed B-cell suppression earlier, in which both the positive and negative regulators of B cells were suppressed within a short time, and the mice underwent senescence that mimicked stromal-cell impairment. TGF-β is produced by stromal cells (25) and is also a negative regulator of B lymphopoiesis (26). Fernandez *et al.* have recently demonstrated that TNF-α has a direct inhibitory effect on IL-7 responses in $B220^+$ /IgM^- pre-B cells (27). Neopterin was found to amplify the secretion of TNF-α from peripheral blood mononuclear cells induced by the lipopolysaccharide (LPS), IFN-γ and IL-2 (28). In addition, in vascular smooth muscle cells, neopterin potentially stimulates TNF-α gene expression and protein release (29). Fernandez *et al.* have recently shown that IL-6 indirectly inhibits IL-7 responses in $B220^+/IgM^-$ B-cell progenitors by inducing the stromal-cell production of an inhibitory factor (27). Furthermore, Nakamura *et al.* (30) and Maeda *et al.* (31) have demonstrated recently that IL-6 suppresses B-cell differentiation and causes excessive myeloid development in BM. When cultured non-SCI stromal cells were treated with neopterin, the negative regulators of the B-cell lineage such as TNF-α, IL-6, and TGF-β were all upregulated significantly, whereas the upregulations of the gene expressions of these cytokines were not observed in cultured senescent SCI stromal cells. Therefore, the milder suppression of B-cell proliferation in the SCI group is assumed to be caused by the age-related functional deterioration of stromal cells.

Next, we examined the effect of neopterin *in vivo* using non-SCI mice. The intraperitoneal administration of neopterin at two doses to the non-SCI mice for three consecutive days resulted in a dose-dependent decrease in the number of femoral CFU-preB cells on Day 1, a finding that was consistent with those of the *in vitro* experiments (Fig. 1). When the non-SCI mice were administered repeatedly with neopterin, the number of CFU-preB cells decreased on Day 1, then rapidly increased to 209% 7 days after the neopterin treatment, and then returned to the level before the treatment (Fig. 3). As a mechanism underlying the decrease in CFU-preB-cell number on Day 1, on the bases of cytokine levels, it can be observed that the negative regulators of B lymphocytes such as TNF-α and IL-6 were predominantly and markedly increased 1 hr after neopterin treatment (Fig. 4B, C). These increases in the levels of negative regulators indicate that TNF-α and IL-6 play key roles as major cytokines in the suppression of B lymphopoiesis *in vivo* 1 day after neopterin treatment. After three consecutive days of treatment, all the cytokine levels decreased after 24 hrs and then started to increase 7 days after the last treatment. As a mechanism underlying the subsequent rapid increase in CFU-preB-cell number, the most important factor contributing to the recovery up to Day 7 from B-cell suppression 1 day after neopterin treatment was the marked downregula-

←

Figure 4. Time courses of IL-7, TNF-α, IL-6, and TGF-β gene expression levels in BM cells from non-SCI and SCI mice after single intraperitoneal injection of 3.5 mg/kg neopterin. Total RNA was extracted from BM cells of the non-SCI and SCI mice (A–D and E–H, respectively) at 30 mins, and 1, 2, 6, and 24 hrs after a single intraperitoneal injection of 3.5 mg/kg body weight neopterin using TRIzol (Invitrogen) according to the manufacturer's instructions. The extracted RNA was reverse-transcribed using Superscript (Life Technologies) and Oligo-dT (Promega). The reverse-transcribed complementary DNAs were then amplified by real-time polymerase chain reaction (real-time PCR) using TaqMan universal PCR master mix (Applied Biosystems) and specific primers for murine IL-7 (A vs. E), TNF-α (B vs. F), IL-6 (C vs. G), TGF-β (D vs. H) and GAPDH. GAPDH gene expression levels are the same in non-SCI and SCI mice (see Appendix). The results are expressed as a ratio to each value of the nontreated non-SCI and SCI group. Each bar represents the mean ± SD obtained from triplicate experiments. $^*P < 0.05$, $^{**}P < 0.005$ vs. each control.

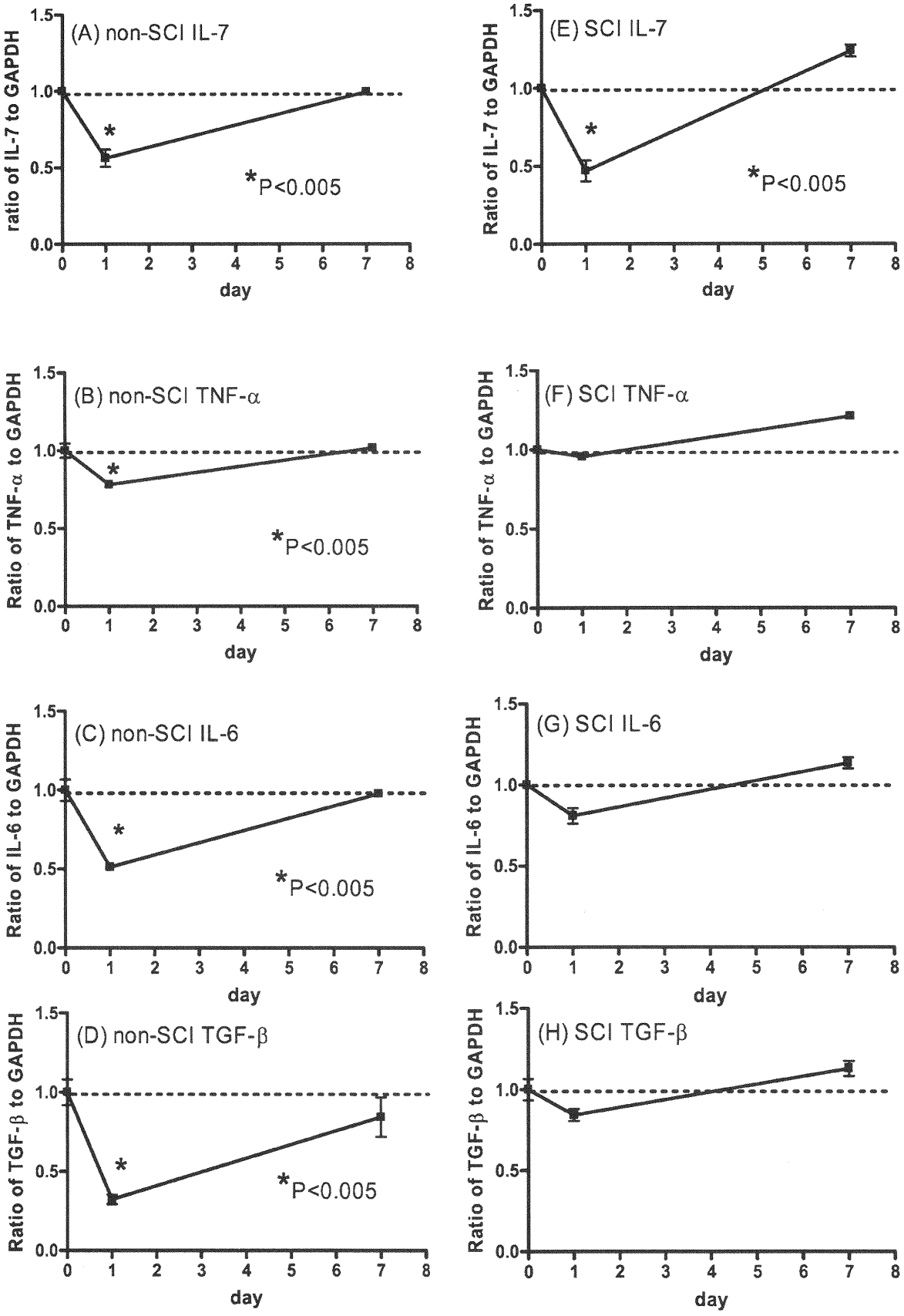
(A) non-SCI IL-7
ratio of IL-7 to GAPDH
*P<0.005
day
(E) SCI IL-7
Ratio of IL-7 to GAPDH
*P<0.005
day
(B) non-SCI TNF-α
Ratio of TNF-α to GAPDH
*P<0.005
day
(F) SCI TNF-α
Ratio of TNF-α to GAPDH
day
(C) non-SCI IL-6
Ratio of IL-6 to GAPDH
*P<0.005
day
(G) SCI IL-6
Ratio of IL-6 to GAPDH
day
(D) non-SCI TGF-β
Ratio of TGF-β to GAPDH
*P<0.005
day
(H) SCI TGF-β
Ratio of TGF-β to GAPDH
day

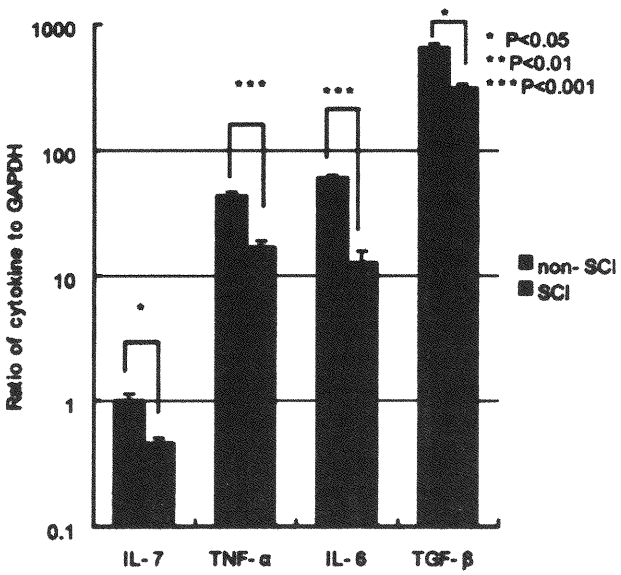

Figure 6. Relative expression levels of positive regulator IL-7, negative regulators TNF-α, IL-6, and TGF-β from non-SCI mice (dark columns) and SCI mice (light columns) (values relative to expression level of IL-7 from non-SCI considered as 1.0). Total RNA was extracted from BM cells of non-SCI and SCI mice using the TRIzol reagent (Invitrogen) according to the manufacturer's instructions. The reverse-transcribed complementary DNAs were then amplified by real-time polymerase chain reaction (real-time PCR) using the TaqMan universal PCR master mix (Applied Biosystems) and specific primers for murine IL-7, TNF-α, IL-6, TGF-β, and GAPDH. The results are expressed as a ratio to the expression level of GAPDH in the cultured non-SCI or SCI fraction. Each bar represents the mean ± SD obtained from triplicate experiments. $^{*}P < 0.05$, $^{**}P < 0.01$, $^{***}P < 0.001$ vs. non-SCI.

tion, on Day 1, of negative regulators, specifically TGF-β (Fig. 5), as compared with the steady-state value (Fig. 6), which could be a potential trigger for the recovery. Throughout the experiment, the expression levels of the genes in the stroma of the SCI mice and the negative regulator cytokines were lower than those in the non-SCI mice. It seems likely that stromal cells that have undergone senescence could not induce TNF-α and IL-6 production in the early phase of neopterin administration and could not suppress TGF-β production in the late phase of neopterin administration, resulting in milder changes in B lymphopoiesis in the SCI mice than in the non-SCI mice. The difference in anti-inflammatory resistances between non-SCI mice and SCI mice has not been tested, but according to references available, a senescent mouse is much more sensitive than a young mouse to a challenge with LPS and TNF-α (32, 33).

These results suggest that the suppression of B cells is milder in the SCI mice, indicating that response of granuloid lineages to suppurative inflammation is very weak. Thus, it is suggested that the hematopoietic regulations during the suppurative inflammatory process in senescence are based on the competitive bilateral regulation between the stimulation of granulopoiesis and the suppression of lymphopoiesis, which forms a hematopoietic environment for anti-inflammatory hematopoietic proliferation. In a senescent hematopoietic environment, it is noted that hematopoietic suppression is not based on the stimulation of the suppression system, but rather on both the positive and negative regulators that are downmodulated simultaneously. Cytokines in homeostasis are at lower functional levels. Therefore, the senescent-downmodulated homeostasis hardly recovers to the upper functional level by a simple administration of one-sided negative or positive regulator. Downmodulated homeostasis is, thus, an important subject of studies in future antisenescent hematologic programs.

Further studies are required to elucidate the mechanisms underlying the neopterin action, but our present findings taken together provide evidence that neopterin is a potent B-lymphopoietic regulatory factor and that the response of B lymphopoiesis to neopterin changes with senescence.

We thank Dr. Yukio Kodama, Ms. Erika Tachihara, Ms. Yoshiko Usami, and Ms. Minako Kenjoh for assistance in maintaining the SAM/P-1 mice in the experimental animal facilities, and Ms. Sonoko Araki and Ms. Sachiko Yuda for technical assistance.

APPENDIX

Glyceraldehyde phosphate dehydrogenase (GAPDH), a housekeeping gene expression in non-SCI (stromal-cell impairment) or SCI steady-state mice.

In the present study, cytokine genes were evaluated quantitatively by real-time PCR using the Taqman Universal PCR master mix and specific primers and probes (see Materials and Methods). Because the expression of each of the cytokines was evaluated as a ratio to the standard expression level of GAPDH from non-SCI mice and SCI mice, respectively, the steady-state expression of GAPDH in non-SCI mice was compared with compatible GAPDH expression level in SCI mice.

Total RNA was extracted from BM cells using TRIzol

←

Figure 5. Time courses of IL-7, TNF-α, IL-6, and TGF-β gene expression levels in BM cells from non-SCI and SCI mice (A–D and E–H, respectively) after intraperitoneal injection of 3.5 mg/kg body weight neopterin for three consecutive days. Total RNA was extracted from BM cells of non-SCI and SCI mice 1 and 7 days after the intraperitoneal injection of 3.5 mg/kg body weight neopterin for three consecutive days using the TRIzol reagent (Invitrogen) according to the manufacturer's instructions. The reverse-transcribed complementary DNAs were then amplified by real-time polymerase chain reaction (real-time PCR) using the TaqMan universal PCR master mix (Applied Biosystems) and specific primers for murine IL-7 (A vs. E), TNF-α B vs. F IL-6 (C vs. G), TGF-β (D vs. H) and GAPDH. GAPDH gene expression levels are the same in non-SCI and SCI mice (see Appendix). The results are expressed as a ratio to each value of the nontreated non-SCI or SCI group. Each bar represents the mean ± SD obtained from triplicate experiments ($^{*}P < 0.005$ vs. each control).